

## TABLE OF COMMENTS

<b>ABSTRACT.....</b>	<b>3</b>
<b>1.0 INTRODUCTION.....</b>	<b>3</b>
<b>2. AIRCRAFT REQUIREMENTS.....</b>	<b>4</b>
<b>3. COMPETITOR AIRCRAFTS.....</b>	<b>4</b>
3.1 F-16B Fighting Falcon.....	4
3.2 T50 Golden Eagle .....	4
3.3 Dassault Mirage 2000B.....	5
3.4 HAL Tejas.....	5
3.5 CAC J-10B .....	5
3.6 Mitsubishi F2B .....	6
3.7 JAS Gripen 39B.....	6
3.8 Competitor Aircraft Parameters .....	7
3.9 Geometrical Parameters .....	7
3.10 Performance Parameters .....	7
3.11 Weight of the Competitor Aircrafts .....	7
3.12 Comment About Competitor Aircraft.....	8
<b>4. Take-off Gross Weight Calculation.....</b>	<b>8</b>
4.1 Mission Profile.....	8
4.2 Weight Estimation.....	9
4.3 Empty Weight Fraction.....	9
4.4 Fuel Weight Fraction.....	10
4.5 Payload Weight .....	11
4.6 Results of Trade-off Analysis.....	11
4.7 Comments about Competitor Aircraft.....	12
<b>5. CALCULATION OF AIRFOIL WING VARIABLES.....</b>	<b>12</b>
5.1 Airfoil Selection.....	12
<b>6. AIRCRAFT GEOMETRICAL CHARACTERISTICS AND WING LOADINGS.....</b>	<b>14</b>
6.1 Aspect Ratio .....	14
6.2 Taper Ratio .....	14
6.3 Twist Angle.....	14
6.4 Sweep Angle .....	14

6.5 Mach Critical .....	14
6.6 Wing Loading for Stall Speed.....	15
6.7 Wing Loading For Take-off Distance .....	15
6.8 Wing Loading For Landing Distance.....	15
6.9 Wing Loading For Cruise .....	15
<i>10. Location and sizing of the landing gear.....</i>	<i>22</i>
<i>12.3 Range.....</i>	<i>34</i>
<i>12.4 Endurance .....</i>	<i>35</i>
<i>12.5 Maximum Velocity.....</i>	<i>35</i>
12.6 Stall Speed.....	35
12.7 Take-off and Landing Distance.....	36
12.7.1 Calculation Ground Roll.....	36
12.8 Landing and Ground Roll Calculation.....	36
<i>13. Accelerated Flight Aircraft Performance Analysis .....</i>	<i>37</i>
13.1 V-n Diagram.....	37
<i>14. Stability Analysis.....</i>	<i>37</i>
<i>15. Cost Analysis .....</i>	<i>38</i>
<i>RESULTS.....</i>	<i>39</i>
<i>CONCLUSION.....</i>	<i>42</i>
<i>REFERENCES.....</i>	<i>43</i>
<i>NOMENCLATURE .....</i>	<i>45</i>

# Competitor Jet Trainer Research Report

## Study 1 – Group 5

**Derya Demirel, Rauf Gümüş, Gialtsin Nteli, Büşranur İşiner, Seren İyikasıp, Emre Kamışlı**

### ABSTRACT

This paper, contains about designing a conceptual multifunctional military aircraft with single turbofan engine and also with two pilots by following the rules in the conceptual design steps. Required performance and design parameters of competitor aircraft, the work has been initiated to create an authentic design and to procure reliable data in accordance with this design by studying. Takeoff gross weight and fuel weight required for the aircraft to perform its design mission was calculated and surmounted before handling the process of aircraft sizing. Suitable airfoil selection was selected according to the specific parameters according to the XFLR5. Vital parameters for the wing configuration were successfully carried out with software programming ANSYS. Stability, control and handling qualities were performed by utilizing the XFLR5 program in detail. This project consists of better estimating takeoff weight of a competitor aircraft. Considering final take-off gross weight, new fuel tank location and center of gravity were obtained. 3D drawing of the aircraft was made by using AUTODESK drawing program. Xfoil are selected for 2-D airfoil analysis. Xfoil uses higher order panel method for analyze the potential flow by starting with the stagnation point, boundary layer analysis module steps along the upper and lower surface of the airfoil. Landing and takeoff parameters of the designing aircraft was calculated according to the parameters. V-n diagram was plotted in order to analyze the capability and maneuverability of the aircraft. Flight envelope of the aircraft was curtailed. Also, the stability and cost analysis were carried out. First of all, the feature of the aircraft is examined to compare these features with the requirements. Then, if the aircraft satisfies the requirements, the aircraft can be used. However, if not, then the previous studies must be checked and corrected to satisfy the requirements. For that reason, it can be said that this is the final part of designing an aircraft.

**Keywords:** Conceptual aircraft design , multifunctional military aircraft, performance parameters

### 1.0 INTRODUCTION

Importance of aviation is increased day by day and companies want to design aircrafts with high efficiency and less price. To design new aircraft requires knowledge about the aircraft which was produced up to now. After a good research and elimination between aircrafts trade study about the all disciplines of aeronautical engineering such as aerodynamic, structure, propulsion, stability and control must be conducted to reach desired goal. A fighter aircraft in today's world plays a super significant role by contributing the countries' military power. Every country aims to create their own fighter instead of buying from other countries, since it is a perfect way to prove the development in technological progress of the nation itself. Keeping that in mind, the pilots who are the only decision makers in a flight, also needs to be well enough to carry out what

was asked for the mission and then successfully land its base. Specified of various properties, these engineering miracles are total source of both attack and defence in case of a dangerous situation that may arise. In order to be successful in every flight, these aircrafts are necessary to be designed with impeccable engineering. Fighter aircraft needs to be designed carefully considering its aerodynamics, structure, control and stability which are main criteria of evaluation. Conceptual design, preliminary design and detail design processes are three main stages to carry out respectively in order to create a fighter aircraft. Among these three, the first one; conceptual design is where the overall shape, weight and performance features are formed by obtaining the general layout of the design. In this final report, the steps of conceptual design for a fighter jet were explained elaborately and every detail needed was presented along with the reached results.

## 2. AIRCRAFT REQUIREMENTS

This section of the report contains information about requirements for the intended aircraft. There is information about performance requirements and mission profile. The requirements for the intended aircraft are given below in *Table 1*. All of the conditions are at sea level condition.

**Table 1:**Requirements of the design

<b>Max Cruise Speed</b>	<b>1.4 Mach</b>
<b>Maximum Range</b>	3000 km
<b>Take-off Distance</b>	350 m
<b>Landing Distance</b>	650 m
<b>Service Ceiling</b>	14000 m
<b>Max Climb Rate</b>	190 m/s
<b>G – limit</b>	+8.5/-3.5
<b>Armaments</b>	9 external stores
<b>Crew</b>	2 pilots
<b>Engine</b>	1 x Turbofan with afterburner

## 3. COMPETITOR AIRCRAFTS

This section of the paper contains general information about the seven competitor aircrafts. The geometrical and performance parameters are mentioned below in this title.

### 3.1 F-16B Fighting Falcon <sup>[1][31][32][33]</sup>

F-16B is trainer and light combat aircraft and it developed in Lockheed Martin (General Dynamics) . The primary variant is one single seated light combat aircraft for reconnaissance missions and air defence. But the trainer variant has a two-seat cockpit which is offered with and without the internal gun and multi role radar. Variety of weapons can be carried with F-16B, air to air and air to ground missiles, for example AIM-9 Sidewinder, IRIS-I or AIM-120, AMRAAM are air to air missiles and for air to ground,AGM-65 Maverick; Penguin anti-ship and stand-off missiles such as Taurus; and Runway Denial Bombs, Cluster Bombs, Laser-Guided Bombs, GPS-Guided Bombs, Conventional Drop Bombs 1x20mm M61A1 Gatling-style internal cannon can be installed as an optional choice. The aircraft is powered by a General Electric F110-GE-100 turbofan engine with afterburner or P&W F100-PW-200/220/229.. These aircrafts have a capacity of 1 or 2 pilots. The aircraft has a tricycle landing gear with conventional tail. The wing configuration is

high wing. The three view of the F16-B Fighting Falcon is shown below in *Figure 1*.

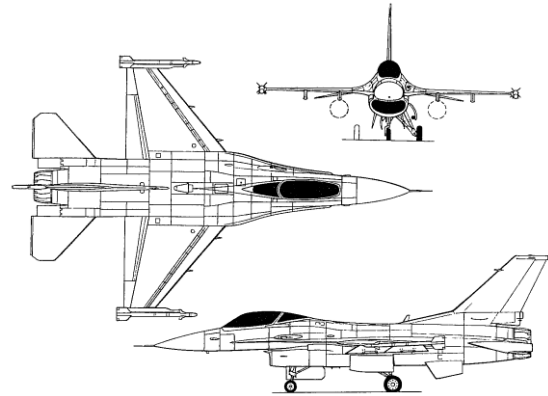


**Figure 1:**F-16B Fighting Falcon 3 side view

### 3.2 T50 Golden Eagle <sup>[3][4][5][6][7][8][9]</sup>

T-50 golden Eagle is also known as the KTX-2 jet trainer and light attack aircraft. It was developed as T-50A advanced trainer and T-50B for fighter trainer versions. This aircraft was built for the republic of Korea Air Force. The first flight of the T-50 was in August 2002. The design of aircraft belongs to Lockheed Martin 13%, Korea Aerospace Industries (KAI) 17% and the government of South Korea 70%. It is powered by a General Electric F404-102 turbofan engine which contains an afterburner. It has seven external hard points for weapons. The aircraft is high wing configuration. Conventional tail configuration. The landing gear of Golden Eagle is tricycle landing gear configuration. The crew number of the aircraft is two. The 3 view of the T50 Golden Eagle is shown below in *Figure 2*.

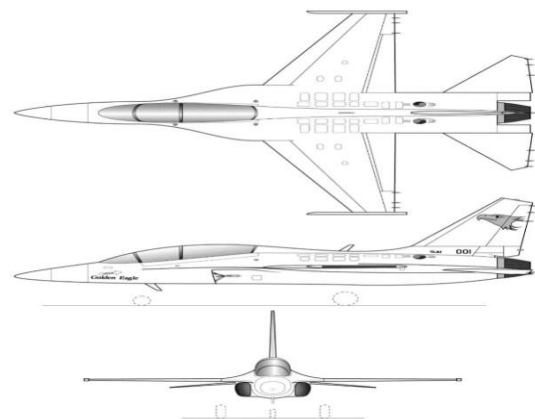


**Figure 2:**T50 Golden Eagle 3 side view

### 3.3 Dassault Mirage 2000B<sup>[10][11][12][13][14]</sup>

Mirage 2000B is the variation of the original Mirage-2000 aircraft which is multirole, has a single engine fourth generation aircraft. Manufacturer of Mirage 2000 is “Dassault Aviation”. The first flew of the Dassault Mirage 2000 is in 1978 it was a fighter. Then making some changes on the Mirage 2000 model some variants of Mirage 2000 manufactured. The trainer variation of the Mirage 2000 is named Mirage 2000B. The Mirage 2000B is two seats is settled and lengthened version of Mirage 2000, is shown in the sky in the 1980. The most interested aspects of Mirage 2000 are that it can combat and perform under extremely hard conditions. Nowadays more than six hundred Mirage 2000 and variants has been manufactured and distributed different countries so It can be seen anywhere around the world. The Mirage 2000 and its variants are in use in the French Air Force and other countries which bought it, they are really effective components of the French Air Force and other countries’ air forces. Mirage 2000B is using turbofan engine with afterburner. Mirage 2000B is low wing configuration. The tail configuration is conventional tail. Landing gear is tricycle configuration.

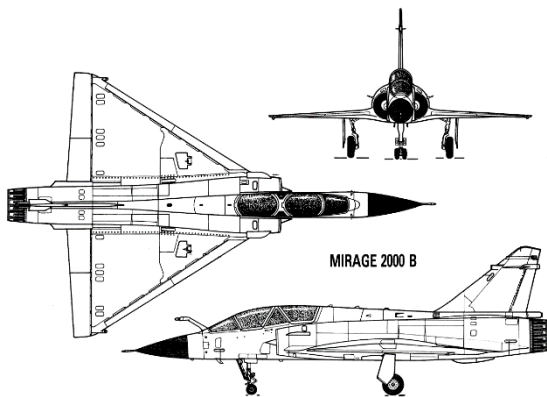


Figure 3: Mirage 2000B three side view

### 3.4 HAL Tejas<sup>[15][16][17][18][19][20][21][22]</sup>

TEJAS is a multi-role combat aircraft which was produced by Hindustan Aeronautics Limited. Design of TEJAS was completed in 1990 and its maiden flight took place in 2007. It entered service in 2016. The TEJAS firstly produced as a single seater, then two-seater variant of TEJAS was produced as a trainer variant. Trainer variant of TEJAS also now in service. The aircraft has delta wing and single

vertical fin. It does not have tail planes and foreplans. TEJAS has modern design concepts such as multi-mode radar (MMR), laser designator pod (LDP), forward looking infrared (FLIR), static instability system, digital fly-by-wire flight control system, HOTAS (hands-on throttle and stick), and microprocessor to carry out the brake system. By using multi-mode radar (MMR), laser designator pod (LDP), forward looking infrared (FLIR) and another opto-electronic sensor accuracy of target stage is increased. At penetration and combat stage ring laser gyro (RLG), inertial navigation system (INS), advanced electronic warfare system (EW) is increased the capability of the TEJAS. As armaments, the TEJAS can carry 8 external stores. 3 of them found on the right side of the wing three of them found on the left side of the wing, one of them found at the center of the fuselage and the remaining one found under the air intake on the port side. The aircraft can carry air-to-air, air-to-ground, and ship missiles, precision-guided munitions, bombs and rockets. In addition, Derby BVR missile, Vamped R-37. TEJAS is powered with GE F404-GE-IN20 turbofan engine with afterburner. The figure of the aircraft is shown below in Figure 4.

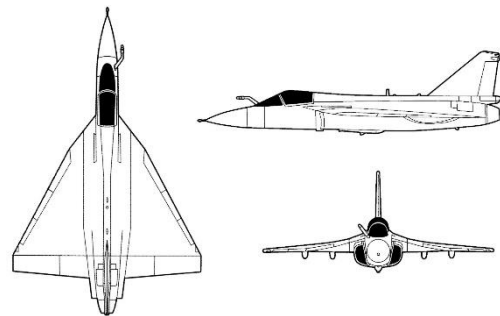
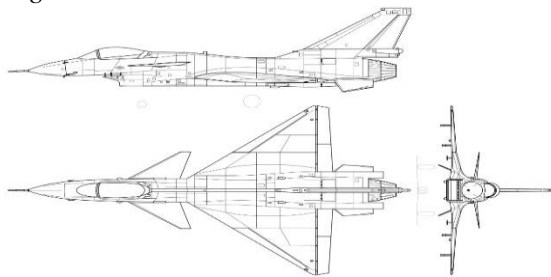


Figure 4: HAL Tejas three side view

### 3.5 CAC J-10B<sup>[23]</sup>

CAC J-10 is a multirole fighter aircraft which was produced by Chengdu Aircraft Corporation and 611 Institute. In the mid of 1980, study and projects were started about J-10 and the first flight of single seat variant took place in 1988. In addition, dual seat version of J-10B was produced as a training variant. First flight of that dual seat version took place in 2003. Single and dual seat version of J-10 was entered in service in 2005. The design of that aircraft is based on low

mounted delta wing, front canard wing and a large vertical fin and two under fuselage wing. Because of unstable design aircraft controlled with computerised digital fly-by-wire system and HOTAS (hands-on throttle and stick). In addition, J-10 equipped with forward-looking infrared and laser target designator pod sensor to give motion capability to weapons. The aircraft has 11 store station. Five of the stores is under the fuselage and the remaining stores are under the wing. It carries air to air missiles and these are PL-8, PL-9, Python-4, R-73, R-77. Also, Laser-guided bomb, YJ-81 (C-801) anti-ship missile are the ground attack weapons. As an engine, single AL-31F turbofan with afterburner. The three-view image of the CAC J-10B is shown below in *Figure 5*.



**Figure 5:**CAC J10B three side view

### 3.6 Mitsubishi F2B<sup>[24][25][26][27]</sup>

Mitsubishi Heavy Industries' F-2 fighter looks a lot like the Lockheed Martin F-16, because the company developed the indigenous type in cooperation with the US manufacturer. Japan's air force today flies 63 F-2A-model examples and 15 two-seat F-2B trainers. F-2 landing gear system has retractable tricycle type, with single wheel on each unit; main wheels retract inward, nose wheel rearward. The wing configuration of F2B is low wing. The tail is conventional. It is powered with General Electric F110-GE-129 turbofan engine with afterburner. F2B is multirole aircraft main is used as a jet trainer aircraft. F2B could carry thirteen external stores and one internal store. The three view of the Mitsubishi F2B is shown below in *Figure 6*.

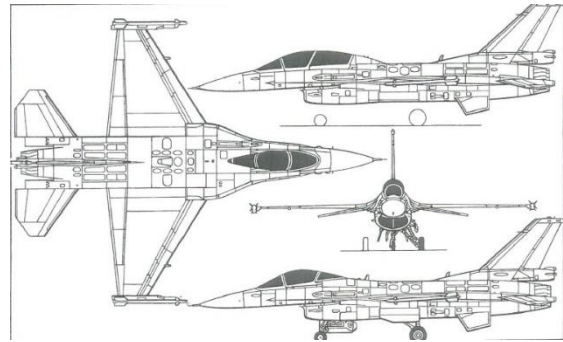


**Figure 6:**Mitsubishi F2B three side view

### 3.7 JAS Gripen 39B<sup>[28][29][30]</sup>

JAS 39B Gripen is a multi-role combat aircraft which was produced by Saab Military Aircraft, Ericsson Microwave Systems, Volvo Aero Corporation and Celsius Aerotech. JAS 39B Gripen is a two-seater operational trainer variant. The JAS 39B has same avionics and weapons with its single seat variant JAS 39A. Difference of the JAS 39B from JAS 39A is exception of gun. The aircraft has delta wing and canard configuration. The flight control system of that aircraft is a triplex digital fly-by-wire system and HOTAS (hands-on throttle and stick). Also, JAS 39B includes The Ericsson PS-05 long-range multi-purpose pulse Doppler radar that helps long range area investigation and targeting. Forward-looking infrared (FLIR) sensor is used at that aircraft. As an armament, advanced medium range air to air missiles, sidewinder short range air to air missiles, sea-skimming ant ship missiles, advanced dispenser weapon systems, air to ground weapons (Maverick, rocket pods), active/passive warfare electronic system, internal and external reconnaissance systems are available. JAS 39 Gripen is powered with Volvo Aero RM12 turbofan with afterburner. The three-view figure of aircraft in shown below in *Figure 7*.

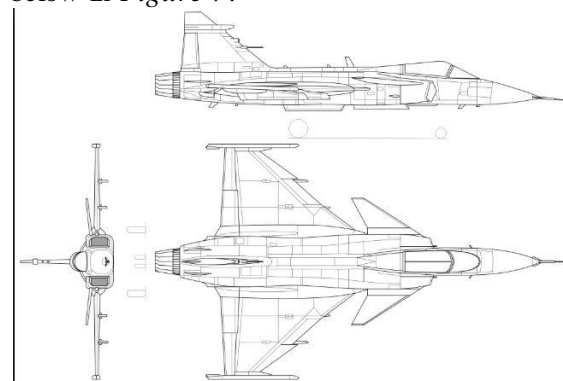


**Figure 7:** JAS Gripen 39B three side view

### 3.8 Competitor Aircraft Parameters

This section of the report contains detailed information about the researched aircraft. The content of the tables is about weight, geometrical and performance parameters.

### 3.9 Geometrical Parameters

This section of the report contains information about geometrical parameters of competitor aircrafts. The parameters are shown below in *Table 2*.

**Table 2:**Geometrical Parameters of Competitor Aircraft

Airplane Model	Wingspan(m)	Length (m)	Height (m)	Wing Area (m <sup>2</sup> )	Aspect Ratio
F16-B Fighting Falcon	9.449	15.027	5.090	27.87	3.20
T50 Golden Eagle	9.11	12.98	4.78	23.69	3.50
Dassault Mirage 2000B	9.13	14.55	5.15	41	2.03
HAL Tejas Mk 1	8.2	13.2	4.4	38.4	1.75
CAC J-10B	8.78	14.57	4.78	33.1	2.32
Mitsubishi F2B	10.8	15.52	4.96	34.84	3.34
JAS 39B	8.4	14.1	4.5	30	2.35
<b>Averages</b>	<b>9.00</b>	<b>14.095</b>	<b>4.72</b>	<b>32.53</b>	<b>2.55</b>

### 3.10 Performance Parameters

This section of the report contains information about performance parameters of competitor aircrafts. The parameters are shown below in *Table 3*.

**Table 3:**Performance Parameters of Competitor Aircraft

Airplane Model	Take-off Distance (m)	Landing Distance (m)	Service Ceiling (m)	Max Climb Rate (m/s)	Max Speed (km/h)
F-16B Fighting Falcon	345	457	15240	254	2450
T50 Golden Eagle	400	520	14630	198.12	1837
Dassault Mirage 2000B	503	610	16470	284.483	2338
HAL Tejas Mk 1	396	600	15240	N/A	2000
CAC J-10B	350	N/A	18000	N/A	2450
Mitsubishi F2B	N/A	N/A	18000	243	2500
JAS 39B	400	500	15240	N/A	2470
<b>Averages</b>	<b>399</b>	<b>537.4</b>	<b>16117.14</b>	<b>244.90</b>	<b>2292.1</b>

### 3.11 Weight of the Competitor Aircrafts

This section of the report contains information about the weight of the competitor aircraft that shown in the *Table 4*.

**Table 4:Weights of Competitor Aircraft**

Airplane Model	MTGW(kg)	Empty weight (kg)
F-16B Fighting Falcon	21772	9027
T50 Golden Eagle	13471	6263
Dassault Mirage 2000B	17000	7500
HAL Tejas Mk 1	13300	6560
CAC J-10B	18400	9750
Mitsubishi F2B	13230	9633
JAS 39B	18500	9750
<b>Averages</b>	<b>16524</b>	<b>8354.7</b>

### 3.12 Comment About Competitor Aircraft

The best aircraft are chosen by considering geometric parameters, performance parameters and weights of competitor aircraft. The specifications of the competitor aircraft are listed in the *Table 2*. When designing aircraft, geometric features have an enormous crucial that affects the performance of the aircraft. The selections of the competitor aircraft are important since the competitor aircraft gives the idea about the way of to reach desired parameters of aircraft. After observations and compares each other between competitor aircraft. As it is seen at the *Table 2*, the wing area of KAI T-50 Golden Eagle is considerably smaller than other aircraft. For F16-B Fighting Falcon, The greatest maximum takeoff weight between competitors, is on F16-B Fighting because it's external fuel tank is the biggest one. The closest parameters that are desired to reach with designed aircraft are found on KAI T-50 Golden Eagle which is multi-role aircraft.

## 4. Take-off Gross Weight Calculation

### 4.1Mission Profile

This section of the report contains information about the mission profile of the aircraft. Mission profile of an aircraft leads the design. The major parameters are cruise range, combat duration, loiter duration and altitude. The intended design will be shaped with these parameters. The following figure shows the mission profile for the intended jet trainer design.

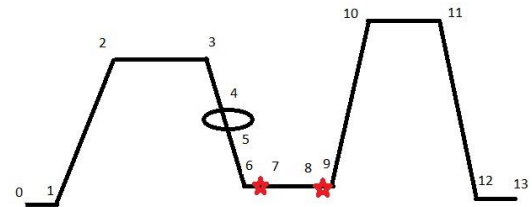


**Figure 8:Mission Profile**

The figure shows the steps of the mission profile. The steps of profile are explained below in *Figure 8*.

**Table 5:Mission Segments.**

Mission Segment	Description
<b>0 – 1</b>	Take-off at sea level
<b>1 – 2</b>	Climb to 8 km
<b>2 – 3</b>	Cruise for 1500 km
<b>3 – 4</b>	Decent to 4km
<b>4 – 5</b>	Loiter for 1 hour
<b>5 – 6</b>	Decent to 1km
<b>6 – 7</b>	Drop 3 air to ground missiles
<b>7 – 8</b>	Dog fight for 10 min
<b>8 – 9</b>	Launch 3 air to air missiles
<b>9 – 10</b>	Climb to 10 km
<b>10 – 11</b>	Cruise for 1500 km
<b>11 – 12</b>	Decent for Landing
<b>12 – 13</b>	Landing

The fuel weight of the aircraft was calculated according to the segments of the mission profile. The details and the equations of the calculations is shown in the next section of the paper.



## 4.2 Weight Estimation

This section of the report explains the details of the weight estimation calculations. The objective function of weight that called weight fractions about mission profile is shown below in following instructions depends on mission segment. The weight fraction from  $\frac{W_1}{W_0}$  to  $\frac{W_6}{W_5}$  and  $\frac{W_9}{W_8} \frac{W_{10}}{W_9} \frac{W_{11}}{W_{10}}$  are calculated by using empirical relations depend on the mission. The obtained values are respectively 0.8545 and 0.9208. Cruise Mach number selected 0.8. After dropping the bombs, our weight fraction becomes;

$$\frac{W_7}{W_6} = \frac{(W_6 - \text{air to ground missiles})}{W_6} \quad (1)$$

After dropping air to ground missiles, the combat starts. The weight ratio of the combat is calculated as 0.85 and our new weight ratio for combat becomes;

$$\frac{W_8}{W_7} = \frac{0.85(W_6 - \text{air to ground missiles})}{(W_6 - \text{air to ground missiles})} \quad (2)$$

at the end of the combat air to air missiles are used. And the new weight ratio;

$$\frac{W_9}{W_8} = \frac{W_8 - \text{air to air missiles}}{0.85(W_6 - \text{air to ground missiles})} \quad (3)$$

And for the second climb weight fraction becomes by multiplication of the weight and using empirical value

$$\frac{W_{10}}{W_9} = \frac{0.74(W_8 - \text{air to ground missiles})}{W_8 - \text{air to ground missiles}} \quad (4)$$

To minimize the unknowns  $W_6$  was obtained as

$$W_6 = W_0 \frac{W_1}{W_0} \frac{W_2}{W_1} \frac{W_3}{W_2} \frac{W_4}{W_3} \frac{W_5}{W_4} \frac{W_6}{W_5} \quad (5)$$

$W_6 = 0.8545W_0$  and  $W_6$  is replaced with  $0.8545W_0$

After the calculations the new weight fraction equation becomes;

$$\frac{W_{13}}{W_0} = \frac{W_1}{W_0} \frac{W_2}{W_1} \frac{W_3}{W_2} \frac{W_4}{W_3} \frac{W_5}{W_4} \frac{0.8545W_0 (0.8545W_0 - \text{air to ground missiles})}{0.8545W_0} \quad (6)$$

$$\frac{0.85(0.8545W_0 - \text{air to ground missiles})}{(0.8545W_0 - \text{air to ground missiles})} \frac{W_6 - \text{air to air missiles}}{0.85(0.8545W_0 - \text{air to air missiles})} \frac{W_{11}}{W_{10}} \frac{W_{12}}{W_{11}} \frac{W_{13}}{W_{12}}$$

The term  $\left(\frac{W_f}{W_0}\right)$  is the fuel fraction where could be found from the weight fraction of each segment. The term  $\left(\frac{W_e}{W_0}\right)$  is the empty weight fraction where it is calculated from the empirical equations from by Sadraey<sup>[34]</sup>. The term  $W_{\text{crew}}$  is the number of pilots where was calculated as 85kg for each pilot. The term  $W_{\text{payload}}$  is the missile and ammo.

## 4.3 Empty Weight Fraction

Empty weight fraction was used by Sadraey<sup>[34]</sup>. The equation of the empty weight fraction is shown below in Eq( 7).

$$\frac{W_E}{W_0} = aW_0 + b \quad (7)$$

where  $W_0$  stands for the take-off weight. The term a and b used from the Table 6.

Table 6: Historical Aircraft Data

Aircraft Categories	a	b
Twin turboprop	-8.2 $\times 10^{-7}$	0.65
Jet trainer	1.39 $\times 10^{-6}$	0.64
Jet transport	-7.75 $\times 10^{-8}$	0.576
Business jet	1.13 $\times 10^{-6}$	0.48
Fighter	-1.1 $\times 10^{-5}$	0.97
Long range, long endurance	-1.21 $\times 10^{-5}$	0.95

The data for jet trainer took into consideration and the empty weight fraction was calculated

with respect to the constants. The weight fraction equation was multiplied with 0.9<sup>[34]</sup> because of the composite material. The jet trainer considers to build most of the composite materials due the lightness of the aircraft.

#### 4.4 Fuel Weight Fraction

The fuel weight fraction was calculated with respect to the 13 mission segments where it is

$$\frac{W_f}{W_0} = 1.06 \left( 1 - \frac{W_{13}}{W_0} - \frac{W_p}{W_0} \right) \quad (8)$$

**Taxi and Take-off:** this fraction corresponds to  $\frac{W_1}{W_0}$  and with respect to historical data was takes as 0.98.

**Climb and Acceleration:** weight fraction of the climb are calculated with using Eq. (9).

$$\frac{W_i}{W_{i-1}} = 1.0065 - 0.0325(M) \quad (9)$$

The value M is the Mach number during the climb. The data is shown below in Table 7.

Table 7: Climb Weight Fraction Data

Manoeuvre	Mach Number
Climb1	0.3
Climb2	0.74

The fractions were calculated with respect to these input Mach numbers.

**Cruise:** Weight fractions are  $\frac{W_3}{W_2}$  and  $\frac{W_{11}}{W_{10}}$  were calculated with Eq. (10).

$$\frac{W_i}{W_{i-1}} = e^{\frac{-RC}{V(L/D)_{cruise}}} \quad (10)$$

$(L/D)_{max}$  value was estimated from the historical aircraft data.  $(L/D)_{cruise}$  was calculated by 0.866 to  $(L/D)_{max}$ . R is the range which is given from the mission profile. C is the specific fuel consumption of the engine. V is the velocity which is calculated

from the speed of sound with respect to the altitude. The data for the calculation is shown below in Table 8.

Table 8: Cruise Weight Fraction Data

	Mach	L/D	SFC (1/h)
Cruise 1	0.8	15	0.7
Cruise 2	0.8	15	0.7

**Loiter:** weight fraction is  $\frac{W_5}{W_4}$  and was calculated with Eq(11).

$$\frac{W_i}{W_{i-1}} = e^{\frac{-EC}{(L/D)_{max}}} \quad (11)$$

the value E is endurance which loiter duration, C is the specific fuel consumption of the engine and  $(L/D)_{max}$  is takes from the historical data. The values for loiter calculation are shown below in Table 9.

Table 9: Loiter Weight Fraction Data

	SFC (1/h)	L/D	Mach
Loiter	0.8	17	0.38

**Combat:** weight fraction is  $\frac{W_8}{W_7}$  and was calculated by using Eq(12).

$$\frac{W_i}{W_{i-1}} = 1 - c \left( \frac{T}{W} \right) d \quad (12)$$

the term c is specific fuel consumption of the engine, d is the duration and T/W ratio was calculated with Eq(13), (14) and (15).

$$\frac{T}{W} = \frac{qC_{D0}}{W/S} + \frac{W}{S} \left( \frac{n^2}{q\pi A R e} \right) \quad (13)$$

$$\frac{W}{S} = \frac{(T/W) \pm \sqrt{(T/W)^2 - (4n^2 C_{D0} / \pi A R e)}}{2n^2 / q\pi A R e} \quad (14)$$

$$e = 4.61(1 - 0.045AR^{0.68})(\cos\Lambda_{LE}^{0.15}) - 3.1 \quad (15)$$

The T/W ratio was obtained by calculating  $E_q$ ( 14)and( 15). The value  $e$  is Oswald wing efficiency which is dependent of aspect ratio and sweep angle. The aspect ratio and wing loading were taken from the average competitor aircrafts. Sweep angle,  $C_{D0}$ was calculated with respect to the Mach number the equation was takes from the historical data. The value  $n$  load factor was given from the requirements of the aircraft. Wing efficiency was decreased due to the manoeuvres. The effect of acceleration was considered before the combat and the overall fraction was added to the segment. The data in order to calculate the dog fight or combat weight fraction is shown below in *Table 10*.

**Table 10:Dog Fight Fraction Data**

	<b>Dog Fight</b>
<b>SFC - 1/hr</b>	1.080
<b>T/W</b>	0.8612
<b>W/S - <math>kg/m^2</math></b>	142.242
<b>AR</b>	3.8
<b><math>e</math></b>	0.621
<b><math>n</math></b>	6
<b>Sweep Angle - deg</b>	33.3

**Decent and Landing:** weight fractions are  $\frac{W_4}{W_3}$ ,  $\frac{W_6}{W_5}$ ,  $\frac{W_{12}}{W_{11}}$  and  $\frac{W_{13}}{W_{12}}$  were taken as constant of 0.99 according to the historical data.

#### 4.5 Payload Weight

Payload weight of the aircraft with respect to the requirements, the aircraft should contain 9 stores. Four of the stores should be L-Umtas, three of them must be air to air. The remaining two missile are optional. The aircraft might be able to carry two of MK-82 or MK-83. The payload configuration of the aircraft is shown below in *Table 11* ,*Table 12* and *Table 13*

**Table 11:Payload Configuration 1**

<b>Number of Payload</b>	<b>Unit Weight</b>	<b>Total Weight</b>
<b>4 x L-Umtas</b>	37.5	150
<b>3 x Gokdogan</b>	85	255
<b>2 x MK-82</b>	227	454
<b>1 - Ammo</b>	200	200
	<b>Total Weight</b>	<b>1059</b>

**Table 12 Payload Configuration 2**

<b>Number of Payload</b>	<b>Unit Weight</b>	<b>Total Weight</b>
<b>4 x L-Umtas</b>	37.5	150
<b>2 x Gokdogan + 1 x Bozdogan</b>	85-157	327
<b>MK-83 + MK-82</b>	454 -227	681
<b>1 - Ammo</b>	200	200
	<b>Total Weight</b>	<b>1358</b>

**Table 13:Payload Configuration 3**

<b>Number of Payload</b>	<b>Unit Weight</b>	<b>Total Weight</b>
<b>4 x L-Umtas</b>	37.5	150
<b>3 x Bozdogan</b>	157	471
<b>2 x MK-83</b>	454	908
<b>1 - Ammo</b>	200	200
	<b>Total Weight</b>	<b>1729</b>

The tables indicate the payload configuration for the jet trainer aircraft. The selection of two MK-82, MK-83 are due to the stability issues. In order to balance the Center of Gravity (C.G.) the remaining two stores should be selected symmetric in order to provide the stability of C.G.

#### 4.6 Results of Trade-off Analysis

This section of the report contains information about the results of the calculations. During the trade-off studies the payload and range compared with max take-off weight. The effect payload weight and range were calculated by using  $E_q$  (6).The estimated empty weight, fuel weight and maximum take-

off weight is shown below in *Table 14* and 10. The effect of payload weight and range is effect was shown below in *Figure 9* and *Figure 10*

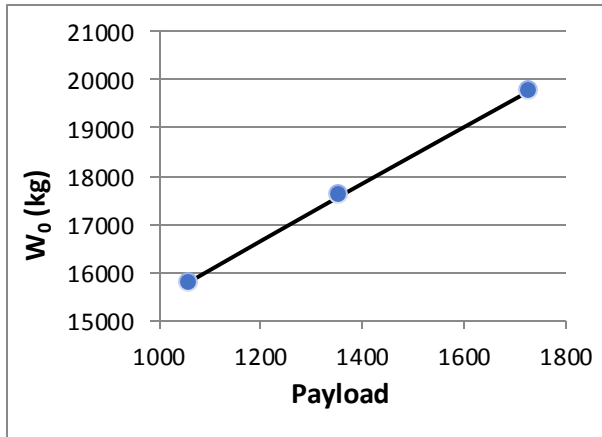


**Figure 9:** Take-off Weight vs Payload graph

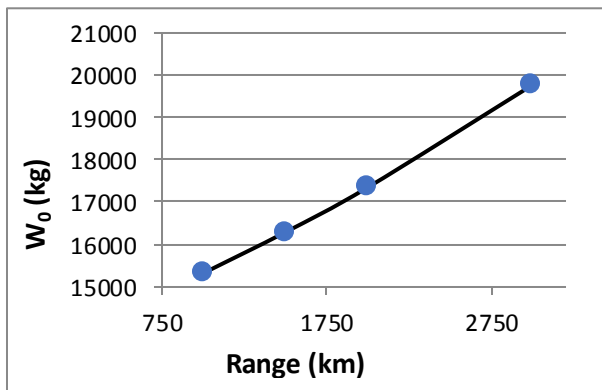


**Figure 10:** Take-off Weight vs Range graph for payload 1729 kg.

**Table 14:** Payload trade off results.

Payload(kg)	$W_f$	$W_e$ (kg)	$W_0$
1059	5683,57	8883,98	15796,55
1358	6308,55	9756,98	17593,54
1729	7070,46	10797,63	19767,09

**Table 15:** Range trade off results for payload 1729 kg.

Range(km)	W(kg)	$W_e$ (kg)	$W_0$
1000	4764,27	8644,17	15307,44
1500	5261,54	9120,63	16281,18
2000	5807,67	9635,67	17342,35
3000	7070,46	10797,63	19767,09

#### 4.7 Comments about Competitor Aircraft

The best aircraft are chosen by considering geometric parameters, performance parameters and weights of competitor aircraft. The specifications of the competitor aircraft are listed in the *Table 2*. When designing aircraft, geometric features have an enormous crucial that affects the performance of the aircraft. The selections of the competitor aircraft are important since the competitor aircraft gives the idea about the way of to reach desired parameters of aircraft. After observations and compares each other between competitor aircraft. As it is seen at the *Table 2*, the wing area of KAI T-50 Golden Eagle is considerably smaller than other aircraft. For F16-B Fighting Falcon, The greatest maximum takeoff weight between competitors, is on F16-B Fighting because it's external fuel tank is the biggest one. The closest parameters that are desired to reach with designed aircraft are found on KAI T-50 Golden Eagle which is multi-role aircraft.

### 5. CALCULATION OF AIRFOIL WING VARIABLES

#### 5.1 Airfoil Selection

Selecting an airfoil is one of the most important part of designing an aircraft. When designing an airfoil it has to be considered that the designing properties and requirements are changing at subsonic and supersonic flights. This report is about the flight regime that contains subsonic and supersonic speeds. That is why the airfoil and its properties were chosen at the optimum values for calculated criteria which are maximum lift coefficient, ideal lift coefficient, and lowest minimum drag coefficient. Highest lift to drag ratio, highest lift curve slope, proper stall qualities were in the stall region. It is also important that the chosen airfoil is able to fly at supersonic speed beside this properties.<sup>[34]</sup> Mach number is obtained 0.3 in the following .

$$Re = \frac{\rho * V_{\infty} * c}{\mu} \quad (16)$$

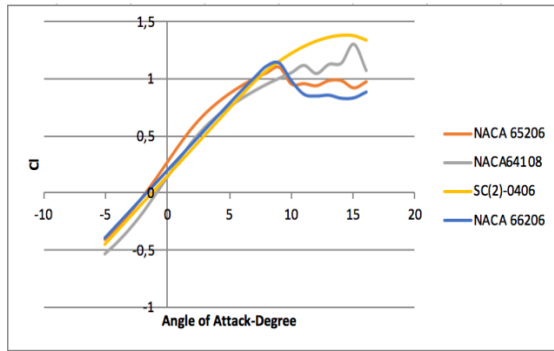


**Figure 11:**  $C_l$  vs Angle of Attack Graph

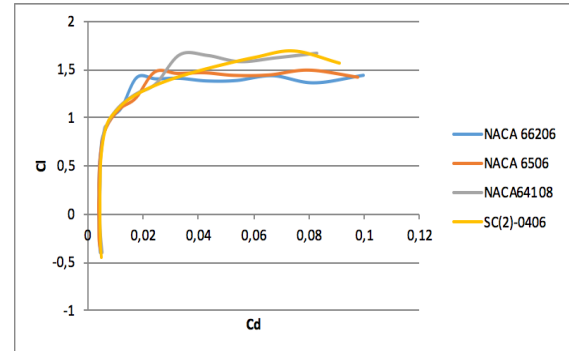


**Figure 15:**  $C_l$  vs  $C_d$  Graph

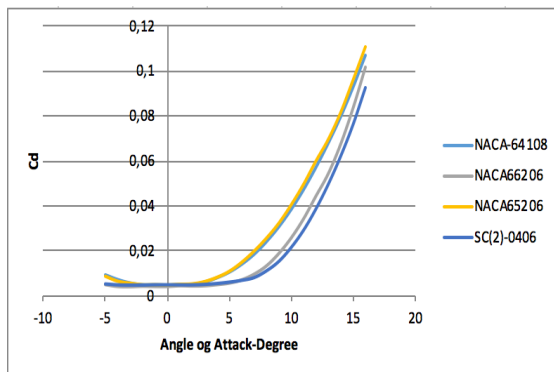


**Figure 12:**  $C_d$  vs Angle of Attack Graph

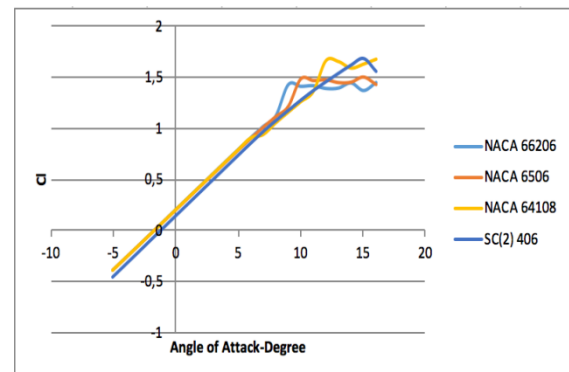


**Figure 16:**  $C_l$  vs Angle of Attack

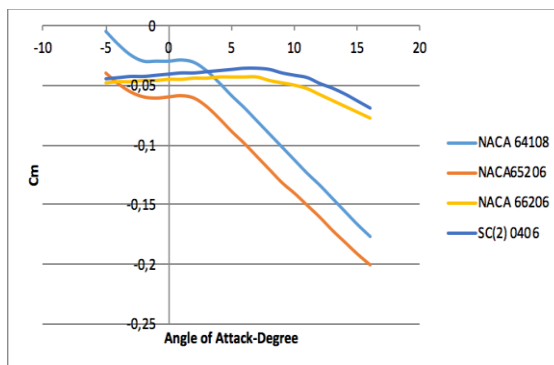


**Figure 13:**  $C_m$  vs Angle of Attack

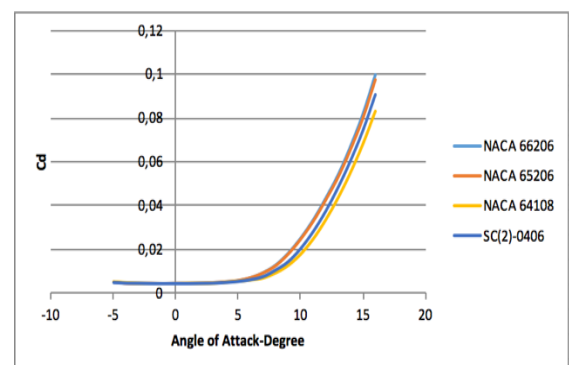


**Figure 17:**  $C_d$  vs Angle of Attack

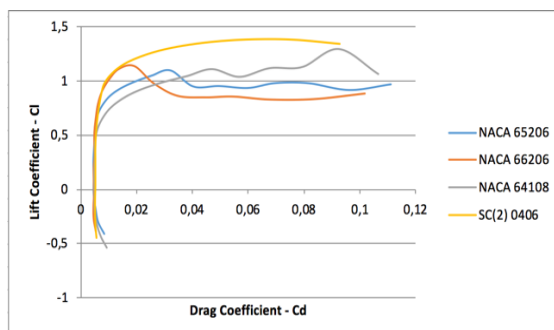


**Figure 14:** Graph of  $C_l$  vs  $C_d$

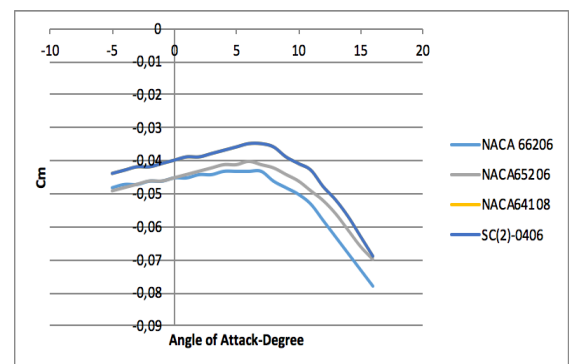


**Figure 18:**  $C_m$  vs Angle of Attack

Mach number in the following Figure 14 is obtained 0.7.

**Table 16: Result of Airfoils**

Airfoil	Stall Ang	Cl	Cd	Cm	Mcrit	Cl/Cd
NACA65206	9	0,125	0,079	-0,287	0.893	1,579
NACA64108	12	0,181	0,020	-0,178	0.893	9,151
SC(2)-0406	14	0,144	0,046	-0,179	1.023	3,125
NACA66206	14	0,126	0,053	-0,349	0.930	2,370

The airfoil trade off analysis was conducted between the airfoils which are shown in the Table 16. Suitable airfoil was selected as NACA64108. During the airfoil selection the major parameters were stall angle of attack, lift, drag, moment coefficients, critical Mach number and lift coefficient to drag coefficient. The highest lift to drag ratio was selected by comparing with stall angle.

## 6. AIRCRAFT GEOMETRICAL CHARACTERISTICS AND WING LOADINGS

### 6.1 Aspect Ratio

To determine AR, empirical formula for jet trainer, fighter was used<sup>[35]</sup>. Also, aspect ratio of competitor aircraft was found. While aspect ratio chosen, g maneuvers capabilities of aircraft has taken into account. Considering the empirical formula and competitor aircraft value, aspect ratio chosen as 3.8.

$$AR_{jet\ trainer} = 4.737(M_{max}^{-0.979}) \quad (17)$$

$$AR_{dog\ fighter} = 5.416(M_{max}^{-0.622}) \quad (18)$$

$$AR_{other\ fighter} = 4.11(M_{max}^{-0.622}) \quad (19)$$

### 6.2 Taper Ratio

Taper is used to decrease the effect of the drag due to lift. According to historical trend<sup>[35]</sup>, taper ratio of swept wing is between 0.2 and 0.3. The taper ratio at that study estimated as 0.2.

### 6.3 Twist Angle

Twist is the important parameter to avoid tip stall and uncontrollable roll moment due to tip loss effect. To make design and manufacturing process easy aerodynamic twist is not used.

Considering the aerodynamic effect of airflow and stability, geometric twist was used. Tip twist is generally between 0 and -5 degree<sup>[3]</sup>. Considering the twist value of jet trainer aircraft, tip twist accepted as -2 degree.

### 6.4 Sweep Angle

Sweep angle is used to postponed the shock wave and decrease the effect of transonic and supersonic flow. At supersonic speeds, to decrease the loss of lift, leading edge of the wing is swept aft of Mach cone angle( $\mu$ ).

$$\mu = \arcsin[1/M] \quad (20)$$

Sweep angle is measured from span wise direction. Leading edge sweep angle was calculated as shown in Eq. (21)<sup>[35]</sup>. Mach cone angle is for maximum speed requirement it will take a little time (dogfight) so it is selected for 1.1-1.2 mach cone condition that  $\frac{3}{4}$  times of the mach cone angle for 1.4 mach speed. It results 33.3 degree.

$$\Lambda_{LE} = 90 - \mu \quad (21)$$

$$\tan \Lambda_{LE} = \tan \Lambda_{c/4} + [(1 - \lambda)/(AR(1 + \lambda))] \quad (22)$$

**Table 17: Mach Cone Angle and Sweep Angle**

<b>Mach Cone Angle(Degree)</b>	44.4 <sup>0</sup>
<b>Sweep Angle at LE(Degree)</b>	33.3 <sup>0</sup>
<b>Sweep Angle at C/4 (Degree)</b>	25 <sup>0</sup>

### 6.5 Mach Critical

The Mach critical ( $M_{crit}$ ) was calculated with the empirical Eq. (24).<sup>[4]</sup> where  $M_{dd}$  is Mach divergence number.

$$M_{dd} = \frac{K_A}{\cos \Lambda} - \frac{t/c}{\cos^2 \Lambda} - \frac{c_l}{10 \cos^3 \Lambda} \quad (23)$$

$$M_{crit} = M_{dd} - \left(\frac{0.1}{80}\right)^{1/3} \quad (24)$$

$$K_A = 0.87 \text{ for NACA 6 digit airfoils}$$

$$K_A = 0.95 \text{ for Super critical airfoils}$$

### 6.6 Wing Loading for Stall Speed

Wing loading for stall speed was calculated by using maximum lift coefficient as shown in Eq. ( 25) and average stall speed of competitor aircraft that is 43.88 m/s was taken into account as shown in Eq. ( 26)

$$C_{L_{\max}} = \frac{2W_{TO}}{\rho V_S^2 S} \quad (25)$$

$$W/S = \frac{1}{2\rho V_{\text{stall}}^2 C_{L_{\max}}} \quad (26)$$

### 6.7 Wing Loading for Take-off Distance

W/S takeoff is calculated with using the Eq. ( 27) given below using the Figure 5.4<sup>[35]</sup> from Raymer's book.

$$W/S_{\text{takeoff}} = (TOP)\sigma_{CLTO} \left( \frac{T}{W} \right) \quad (27)$$

### 6.8 Wing Loading for Landing Distance

W/S landing is obtained by multiplying weight fraction found from takeoff until landing with W/S value for takeoff found before as it is seen Eq.( 28).

$$W/S_{\text{landing}} = W/S_{\text{takeoff}} * W_{\text{landing}}/W_{\text{takeoff}} \quad (28)$$

### 6.9 Wing Loading for Cruise

W/S cruise is calculated by using the Equations ( 29)( 30)( 31) and ( 32) given below.

$$C_{D0} = \frac{S_{\text{wet}}}{S_{\text{ref}}} * C_{fe} \quad (29)$$

$$q_{\infty} = \frac{1}{2} \rho V_{\infty}^2 \quad (30)$$

$$e = 4.61(1 - 0.045AR^{0.68})(\cos\Lambda_{LE}^{0.15}) - 3.1 \quad (31)$$

$$W/S = q_{\infty} \sqrt{\frac{\pi A e C_{D0}}{3}} \quad (32)$$

### 6.10 Wing Loading for Instantaneous Turn Rate

W/S for instantaneous turn calculated by using Eq. ( 33) with using the corner speed which is about 590.5 ft/s.

$$W/S = q_{\infty} \frac{C_{L_{\max}}}{n} \quad (33)$$

### 6.11 Wing Loading For Sustained Turn Rate

W/S for sustained turn is obtained by using Eq. ( 34) with applied reduction one %30 for high g turns.

$$\frac{W}{S} = \frac{(T/W) \pm \sqrt{(T/W)^2 - (4n^2 C_{D0}/\pi A Re)}}{2n^2/q\pi A Re} \quad (34)$$

### 6.12 Suitability of Thrust to Weight to Wing Loading

The suitability of the thrust to weight calculated in the previous parts is compared with the values of other thrust to weight from combat condition in sustained turn and the thrust to weight ratio from wing loading of take-off condition. Along with the distinct results for wing loading of takeoff position obtained from missions, the best one was selected to calculate wing loading in combat position so that thrust to weight for combat and takeoff can be obtained at the end. Wing loading values of each mission was divided to weight fractions before the W/S which is checking in order to obtain wing loading value at takeoff. The results appeared as follows; 86.48 (cruise @8000m), 95.18 (cruise @10000m), 60.17 (instantaneous), 34.59 (sustained). W/S for take-off 86.48 cruise(@8000m) was selected due to being good enough that it can be used for further calculations.

**Table 18:** T/W and W/S results

Missions	W/S (lb/ft <sup>2</sup> )	T/W	W/S (TO)
Take-off	94.17	1.24	-
Cruise(@8000m)	84.47	-	86.48
Cruise(@10000m)	66.55	-	95.18
Stall	42.11	-	-
Instantaneous	50.67	0.86	60.17
Sustained	29.13	-	34.59
Landing	59.96	-	-

## 7. PROPULSION

### 7.1 Thrust to Weight Ratio

Thrust to weight ratio is important for aircraft performance because the ratio is directly proportional to the acceleration of aircraft. So, if thrust to weight ratio increases, aircraft accelerates more quickly, climb more rapidly (high value of excess thrust), reach a higher maximum speed and sustain higher turn rates. If  $T/W$  is greater than one like fighter aircrafts and drag is small, the aircraft can accelerate straight up like a rocket.  $T/W$  is not constant during flight. Thrust depends on the airspeed, altitude and air temperature. In addition, weight depends on the burning fuel and payload. Therefore, during sea level static (zero velocity), standard day condition at design takeoff weight and maximum throttle setting should be prefer for choosing  $T/W$ . For better initial estimate of  $T/W$ , cruise condition can be used. In steady level flight, thrust must be equal to drag and weight must be equal to lift. In addition, consider the aircraft burn some fuel before cruise condition and selected engine's thrust for cruise can be different than at sea level static condition. Thrust to weight ratio is different for takeoff. The cruise thrust at altitude is less than maximum takeoff thrust at sea level because specific fuel consumption increases if altitude increases. From competitor aircraft; the value is 0.90 and from nonlinear regression, thrust to weight is 0.583. The thrust to weight ratio from historical trend in Raymer's book which is found as 0.791.

### 7.2 Engine Selection

Most important point of selecting an engine is corresponding the thrust according that is needed to succeed the take-off. The take-off weight has been found as 19676 kg. The minimum thrust which is needed of the engine must pass 241kN which is obtained by using maximum thrust to weight ratio. According to this, the turbofan engine with an afterburner Kuznetsov NK-32 has been selected. This engine has a maximum thrust of 245kN which supplies the thrust that is needed. This engine has an overall pressure ratio of 28.4 with a low bypass ratio 1.4. The length of this engine is 6m and has a diameter of 1.46m.

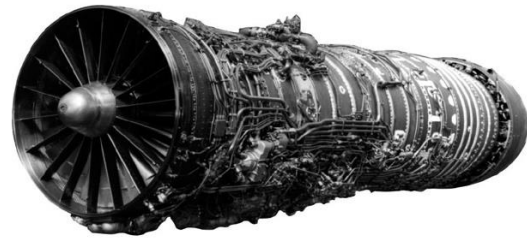


Figure 19: NK-32 Turbofan Engine

### 7.3 Size and Location of the Inlet

Turbofan engines have to slow down the inflow of air to make the air coming to the compressor slower than the sound speed for this reason that engines need to inlet structure. Any inlet must slow the air to about half the speed of sound before it reaches the engine<sup>[1]</sup>. The inlet location can prevent vortex or wake so its location should be selected carefully.

For this design assignment inlet location type is chin type. Chin type inlet are generally use with military aircraft and that has a short duct length. Chin type is good at high angle of attack. These ducts merge before entrance of the engine so this situation provides to minimize the pressure instability risk that can stall the engine. For the stealthiness, radar must not see the engine directly. Therefore, inlet ducts were sized curved for stealthiness purpose. The disadvantages of under wing inlet are location of nose gear which would block and distort the flow.

Capture area ( $A_c$ ) mean inlet entrance area for calculated this area needs to know mass flow rate  $\dot{m}$  and  $A_c/\dot{m}$  ratio. The maximum engine diameter times 0.12 can take instead of mass flow rate. For 1.4 design mach value  $A_c/\dot{m}$  ratio is found 3.65 from following figure.

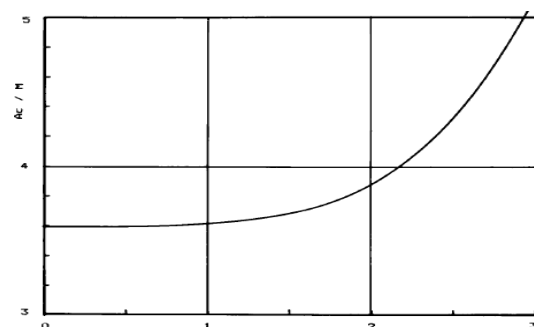


Figure 20: Preliminary capture area sizing



Inlet area distance from the datum point is estimated 6.198 m. Maximum engine diameter is 1460 mm (57.48 in). Capture area is obtained  $0.9216 \text{ m}^2$  and mass flow rate  $604.62 \text{ in}^2$ .

$$\dot{m} = 0.12 * Di^2 \quad (35)$$

$$Ac = 3.65 * \dot{m} \quad (36)$$

## 8. Dimension Calculations of the Aircraft Components

### 8.1 Fuel volume

The volume of the fuel which is calculated with using the weight of fuel and density of fuel. Weight of the fuel which are need to complete mission profile safely are determined before as  $7070,4626 \text{ kg}$ . According to Raymer's book JP-8(Jet A-1) can be used for fighter jet types so it is proper to be selected. JP-8(Jet A-1) have a variable density between 775-840 that can be seen from *Table 19*. To determine the volume for the fuel, density of fuel taken constant fully homogenous density which is assumed that  $820 \text{ kg/m}^3$ . So volume of the fuel calculated as  $8,6225 \text{ m}^3$ .

**Table 19:**Aircraft Fuels

Fuel Type	Density (kg/m3)
Jet A	775-840
Jet A-1	775-840
JP-4	751-802
JP-5	788-806
JP-7	779-806
JP-8	775-840
Gasoline	721-740

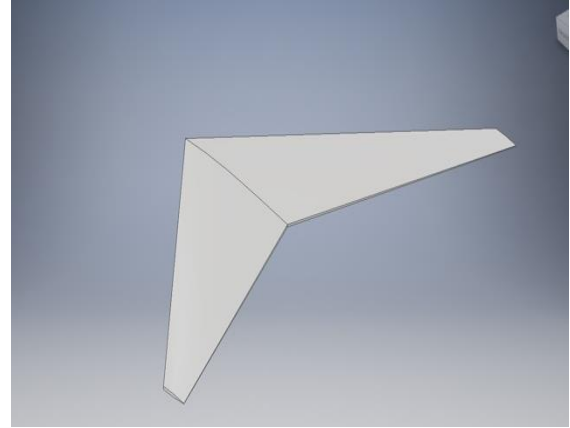


**Figure 21:**Fuel Tank

### 8.2 Wing Sizing

The dimensions of the wing are calculated with using AR and proper maximum W/S which are known that AR is 3.8, W/S value for takeoff is  $86.480$  and the takeoff weight is  $19767.0947 \text{ kg}$  using the equations (37) (38) (39) (40) (41) and (42) dimensions of the wing are calculated. The results of the calculation are shown at *Table 20*.

**Table 20:** Wing Sizing

Dimension Type	Dimension Values
Wing Span	13.3379 m
Wing Area	$46.8157 \text{ m}^2$
Wing Volume	$9.622185 \text{ m}^3$
Fuel Tank Volume	$8.767185 \text{ m}^3$
Fuel Volume	$8,6225 \text{ m}^3$
Root Chord	5.84996 m
Tip Chord	1.16999 m
Mean Chord	3.28598 m
$\bar{Y}$	2.59348 m
Taper Ratio	0.2
Wing Sweep @LE	33.331 deg

$$S = \left[ \frac{W_{takeoff}}{S} \right]^{-1} * W_{takeoff} \quad (37)$$

$$b = \sqrt{AR * S} \quad (38)$$

$$C_{\text{root}} = \frac{2S}{b(1 + \lambda)} \quad (39)$$

$$C_{\text{tip}} = \lambda C_{\text{root}} \quad (40)$$

$$\bar{C} = \left(\frac{2}{3}\right) C_{\text{root}} * \left(\frac{1 + \lambda + \lambda^2}{1 + \lambda}\right) \quad (41)$$

$$\bar{Y} = \left(\frac{b}{6}\right) \left(\frac{1 + 2\lambda}{1 + \lambda}\right) \quad (42)$$

### 8.3 Fuselage

Cabin is designed according to FAA regulations. The common pilot dimensions according to FAA are shown in the *Figure 22*. The seats and initial dimensions of cabin are designed for the type the common pilot according to FAA regulations. Cabin has two seat with 40 degree seat back angle to decrease the diameter and to increase the over nose angle. Both people have a 15 degree over nose angle. In the cockpit the second people which sits back seats have a great view its seat is located higher than first seat. Seats are designed very comfortable as much as possible and cockpit is designed with fifth generation avionics. The exit nozzle is designed with 12 degree decrement with respect to fuselage can be seen *Figure 23*. In addition about the stealthiness, on the empty fraction calculation section the aircraft is designed as a composite so the outer surface material of the aircraft could be that the composite material that have a feature which can absorb the radar signals. Also, aerodynamic considerations of fuselage are taken account for the design. Final 3D drawing of the fuselage is shown in the *Figure 24*.

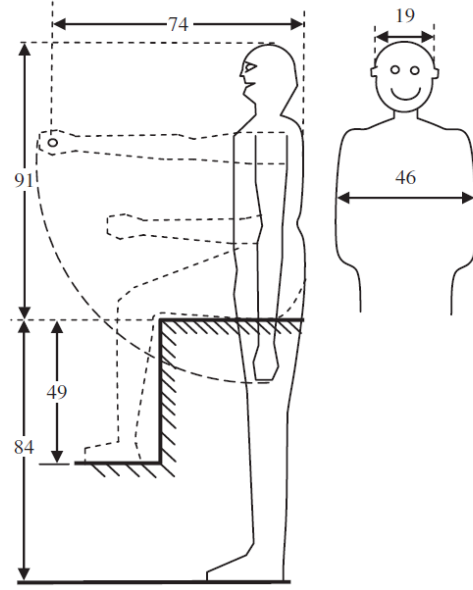


**Figure 22:**Dimensions(cm) of the standard pilot



**Figure 23:** Fuselage nozzle angle

Fuselage length depends on aircraft design takeoff gross weight.

$$l_f = aW_0^c \quad (43)$$

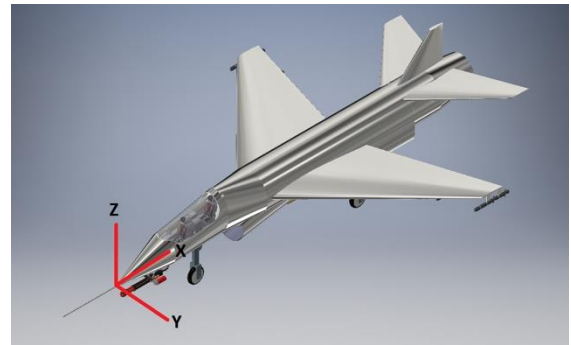


**Figure 24:**Cockpit

For jet trainer a and c values are 0.79 and 0.4 respectively. By using Eq. ( 43 ) length of fuselage calculated as 19.22 meter.

**Table 21 :Fuselage Dimensions**

Dimensions	Values
Fuselage Length	19.22m
Fuselage Diameter	1.95m
Engine Length	6.00m
Engine Diameter	1.46m
Nose Length	5.45m
Cabin Length	3.00m
Cabin Width	1.00m
Seat Width	0.60m
Seat Length	1.2357m
Over Nose Angle for Pilot	15 deg
Over Nose Angle for Student	15 deg
Seatback Angle	40 deg

## 8.4 Wing

Low wing configuration selected for wing vertical location with respect to the fuselage center line. Low wing configuration causes less induced drag. Low wing configuration makes takeoff performance better compared to the mid and high wing. The landing gear is shorter if connected to the wing and this will make the landing gear lighter. Also, the downwash which produced from wing is less which makes the tail more effective. Wing located as horizontally where the center of gravity is 40% of the mean aerodynamic chord.

Wing incidence is the angle between the wing chord and fuselage center line. Most of the military aircraft has no incidence angle and taking into consideration the competitor aircraft incidence angle is selected as  $0^0$ .

Wing dihedral is the angle between the wing and horizontal axis. The primary function of dihedral is to improve the lateral stability of the aircraft. Low wing configuration aircraft has less lateral static stability. Therefore,  $2^0$  is selected as dihedral angle.




**Table 22:Dihedral Guidelines**

	Wing position		
	Low	Mid	High
Unswept (civil)	5 to 7	2 to 4	0 to 2
Subsonic swept wing	3 to 7	-2 to 2	-5 to -2
Supersonic swept wing	0 to 5	-5 to 0	-5 to 0

## 8.5 Tail

Most common type of wing configuration for jet trainer and multirole fighter was observed as conventional tail, v tail, and twin tail.

**Table 23 :Wing Configuration Comparisons**

				
FOM	%FOM	Conventional Tail	V Tail	Twin Tail
Type				
Weight	0.3	0	1	-1
Aerodynamic	0.25	0	1	-1
Stability and Control	0.3	0	-1	1
Manufacturability	0.15	1	-1	1
Total	1	0.15	0.1	-0.5

According to Table 23, conventional tail is selected. Airfoil selection for tail is conducted taken into consideration easy control therefore symmetric airfoil is chosen for tail<sup>[3]</sup>. In addition, thickness of airfoil for tail must be less than wing airfoil. NACA 0006 is selected both horizontal and vertical tail.

## 8.6 Horizontal Tail

Aft portion of the fuselage length taken as 45% of the fuselage length<sup>[1]</sup> and horizontal tail arm considered as equal to the aft portion of the fuselage length as an initial estimation. Dimensions of horizontal tail is calculated by using Equations ( 44 )( 45 ),( 46 ),( 47 ), ( 48 ) and ( 49 ).

$$S_{HT} = \frac{S_w C_{wCHT}}{l_{HT}} \quad (44)$$

$$b_{HT} = \sqrt{AR_{HT} S_{HT}} \quad (45)$$

$$Cr_{HT} = \frac{2S_{HT}}{b_{HT}(1+\lambda_{HT})} \quad (46)$$

$$Ct_{HT} = \lambda_{HT} Cr_{HT} \quad (47)$$

$$\bar{C}_{HT} = \frac{2Cr_{HT}(1+\lambda_{HT}+\lambda_{HT}^2)}{3(1+\lambda_{HT})} \quad (48)$$

$$\bar{Y}_{HT} = \frac{b_{HT}(1+2\lambda_{HT})}{6(1+\lambda_{HT})} \quad (49)$$

In order to avoid shock waves, horizontal tail sweep angle selected higher than wing sweep. Taking into consideration stability effect dihedral and incidence angle selected as 0 degree. Also, volume coefficient, aspect ratio, and taper ratio selected according to jet trainer value<sup>[35]</sup> and the values obtained can be seen in the *Table 24*.

**Table 24:**Horizontal Tail Parameters

Parameters	Value
AR <sub>HT</sub>	3
b <sub>HT</sub>	6.102342 m
λ <sub>HT</sub>	0.3
C <sub>rHT</sub>	3.129406 m
C <sub>tHT</sub>	0.938822 m
$\bar{C}_{HT}$	2.230705 m
$\bar{Y}_{HT}$	1.251762 m
Sweep Angle	37.5°
S <sub>HT</sub>	12.4129 m <sup>2</sup>
l <sub>HT</sub>	8.64885 m
Airfoil	NACA-0006

## 8.7 Vertical Tail

Aft portion of the fuselage length taken as 45% of the fuselage length<sup>[1]</sup> and vertical tail arm considered as equal to the aft portion of the fuselage length as an initial estimation. Dimensions of vertical tail is calculated by using *Equations (50)(51)(52)(53)(54)* and *(55)*.

$$S_{VT} = \frac{S_w C_w c_{VT}}{l_{VT}} \quad (50)$$

$$b_{VT} = \sqrt{AR_{VT} S_{VT}} \quad (51)$$

$$Cr_{VT} = \frac{2S_{VT}}{b_{VT}(1+\lambda_{VT})} \quad (52)$$

$$Ct_{VT} = \lambda_{VT} Cr_{VT} \quad (53)$$

$$\bar{C}_{VT} = \frac{2Cr_{VT}(1+\lambda_{VT}+\lambda_{VT}^2)}{3(1+\lambda_{VT})} \quad (54)$$

$$\bar{Y}_{VT} = \frac{b_{VT}(1+2\lambda_{VT})}{6(1+\lambda_{VT})} \quad (55)$$

In order to avoid shock waves, horizontal tail sweep angle selected higher than wing sweep. Also, volume coefficient, aspect ratio, and taper ratio selected according to jet trainer value<sup>[35]</sup> and the values obtained can be seen in the *Table 25*.

**Table 25 :**Vertical Tail Parameters

Parameters	Value
AR <sub>VT</sub>	1.6
b <sub>VT</sub>	2.63 m
λ <sub>VT</sub>	0.3
C <sub>rVT</sub>	2.53 m
C <sub>tVT</sub>	0.76 m
$\bar{C}_{VT}$	2.00185 m
$\bar{Y}_{VT}$	0.48678 m
Sweep Angle	37.5°
S <sub>VT</sub>	4.33183 m <sup>2</sup>
l <sub>VT</sub>	8.64885 m
Airfoil	NACA-0006

## 8.8 Control Surfaces Sizing

Aileron expand in the range between 50% and 90% of the span generally. In some aircraft

aileron can expand all the way of the span. That extra 10% aileron increases control effectiveness due to vortex flow at the wing tip<sup>[1]</sup>. Also, chord length of the aileron should be in the range between 15% and 30%<sup>[2]</sup>.

Elevator expand in the range between 80% and 100% of the span generally. Also, chord length of the elevator should be in the range between 20% and 40%<sup>[2]</sup>.

Rudder expand in the range between 70% and 100% of the span generally. Also, chord length of the rudder should be in the range between 15% and 40%<sup>[2]</sup>.

Demonstrated that percentage and size of the control surfaces given in the *Table 26*.

**Table 26** :Percentage and size of control surfaces

<b>Aileron</b>	<b>Value</b>
Chord %	20
Span %	90
Root Chord	1.286 m
Tip Chord	0.254 m
Span	6.03 m
Area	4.631m <sup>2</sup>
<b>Elevator</b>	<b>Value</b>
Chord %	40
Span %	100
Root Chord	0.376 m
Tip Chord	1.246 m
Span	3.05 m
Area	2.47 m <sup>2</sup>
<b>Rudder</b>	<b>Value</b>
Chord %	35
Span %	100
Root Chord	0.885 m
Tip Chord	0.245 m
Span	2.63m
Area	1.486m <sup>2</sup>

## 8.9 High Lift Devices

For take-off and landing higher lift can be required. That extra lift provided with the help

of high lift devices. Most fighter and jet trainer use flaperon to reduce weight. Therefore, as a high lift device flaperon is selected.

To sizing the high lift device, lift coefficient of wing is calculated on MATLAB by using lifting line theory. Also, for takeoff required wing lift coefficient is calculated by using *Equations ( 56 ) ( 57 )*.

$$C_{Lmax} = \frac{1.1(W/S)}{g\rho S_g(T/W)} \quad (56)$$

According to required lift flaperon is sized. Flaperon dimensions which is obtained shown in the *Table 27*.

$$\Delta C_{Lmax} = \Delta C_{lmax} \frac{S_{flapped}}{S} \cos \Lambda_{HL} \quad (57)$$

Where  $\Delta C_{lmax}$  is accepted 1.04 for slotted type flap<sup>[1]</sup>.

**Table 27**:Dimensions of flaperons

<b>Flaperon</b>	<b>Dimension</b>
Root Chord	0.254 m
Tip Chord	1.286 m
Span	6.03 m
Area	4.6431 m <sup>2</sup>

## 9. Center Of Gravity Estimation

All the parts of the aircraft is shown in the *Table 28*. The weights of the fuselage, wing, and tail (horizontal and vertical) are calculated respectively with the *Equations ( 58 ) ( 59 ) ( 60 ) and ( 61 )*. For wing aluminum alloy, for horizontal tail graphite epoxy, for vertical tail fiberglass and epoxy glass was selected. Also, for fuselage titanium and aerospace aluminum was used. After calculating the weights, the center of gravity of each part is estimated and located on the aircraft. After the first estimation, changes has been made to find the optimum center of gravity which has to be close to the mean aerodynamic chord. Some parameters were fixed and could not be changed according to the calculations. After adding the landing gear, it has been seen that

the center of gravity moves closer the mean aerodynamic chord which is preferred. The landing gear is placed according to find the optimum center of gravity. after replacing the location of the landing gears. The optimum value was obtained and a better center of gravity estimation has been made that is shown in the *Table 28*.

**Table 28:**Center of Gravity of Each Component of the Aircraft

Part	Weight kg	x (m)	X W	z (m)	z W
Horizontal tail	197.32	17.88	3528.4762	-0.4	-78.928
Vertical tail	55	17.6	968	0.55	30.25
Engine	3500	16.22	56770	0	0
Fuselage	4,177	8.95	37384.15	0	0
Crew	170	3.5	595	0.15	25.5
4*L-Umtaş	150	12	1864.5	-0.48	-72
2*Gökdoğan	170	9.9	1683	-0.48	-81.6
1*Gökdoğan	85	11.5	977.5	-1.43	-121.55
2*Mk-83	908	10	9080	-0.18	-161.62
Ammo	200	2	400	-0.95	-190
Gun	100	2	200	-1.03	-103
Main landing gear	918.83	13.36	12275.568	-2.89	-2655.4
Nose landing gear	334	3.36	1121.3529	2.89	-964.49
Wing	1581	12.08	19098.48	-0.4	-632.4
Total	12,546	140.78	145,946	-10.43	-5,005

**Table 29 :**Center of gravity without landing gear

$X_{cg}$	11.7369
$Z_{cg}$	-0.1226

$$W_w = S_w MAC(t/c)_{max} \rho_{mat} K_{\rho} \frac{AR n_{ult}^{0.6}}{\cos \Lambda_{0.25}} \lambda^{0.04} g \quad (58)$$

$$W_{HT} = S_{HT} MAC_{HT}(t/c)_{max} \rho_{mat} K_{\rho HT} \frac{AR_{HT}^{0.6}}{\cos \Lambda_{0.25}} \lambda_{HT}^{0.04} V_{HT}^{0.3} \frac{C_E}{C_{HT}} g \quad (59)$$

$$W_{VT} = S_{VT} MAC_{VT}(t/c)_{max} \rho_{mat} K_{\rho VT} \frac{AR_{VT}^{0.6}}{\cos \Lambda_{0.25}} \lambda_{VT}^{0.04} V_{VT}^{0.3} \frac{C_R}{C_{VT}} g \quad (60)$$

$$W_F = L_f D_{fmax}^2 \rho_{mat} K_{\rho f} n_{ult}^{0.25} K_{inlet} g \quad (61)$$

$$W_{LG} = K_L K_{ret} K_{LG} W_L \frac{H_{LG}}{b} n_{ultland}^{0.2} \quad (62)$$

The estimation of center of gravity that has been made is calculated without including the landing gear weight which is calculated with Eq ( 62 ). The center of gravity of X-axis and Z-axis was found respectively as 11.7369m and -0.1226m. after these calculations the landing gear has been added the calculation and it is located as 13.36m along the X-axis. the new location of center of gravity shown in the *Table 30*.

**Table 30 :**Center of Gravity with landing gear

$X_{cg}$	11.6329
$Z_{cg}$	-0.3989

**Table 31:**Center of Gravity of Fuel Tank

Part	weight kg	x (m)	X W	z (m)	z W
Fuel tank	7070.46259	12.1	85552.60	-0.4	-2828.18

The new location of center of gravity which is fuel tank and landing gear added can be seen the *Table 32*.

**Table 32:** Center of gravity with landing gear and fuel tank

$X_{cg}$	11.79791
$Z_{cg}$	-0.25519

## 10. Location and sizing of the landing gear

The landing gears provide to make taxi, takeoff and landing of aircraft. In this design tricycle landing gear types are used. Tricycle type one nose wheel is front of the aircraft, two main wheels are aft side of the aircraft like

show as in the *Figure 25*.

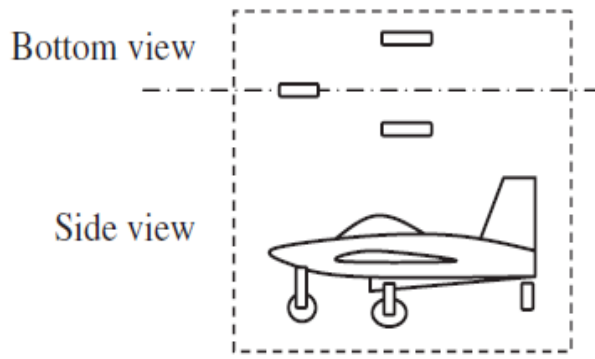


**Figure 25:**Tricycle type landing gear

Total aircraft weight is shared with main and nose gears; main gears are carried the total weight is about 80-90%, nose gear carries about 10-20% <sup>[2]</sup>. The main gears and nose gear have the same height but nose gear is smaller than main gears as 80% percentage.

For this design retractable landing gear is selected. In retractable gear, after takeoff the landing gear is entered the treasure in the aircraft. In low wing configuration retract the main gear also the nose wheel into in fuselage. The advantages of retractable landing gears are less drag and higher aircraft performance. The disadvantages of retractable landing gears are expensive, heavier, harder to design, harder to manufacture, harder to maintain less stable and less available internal fuel volume. Disadvantages are more than the advantages but less drag and higher aircraft performance features are satisfying the others. The clearance is measured from the lowest point of the aircraft to the ground. Recommended clearances shown in the *Table 33*.

**Table 33:**Rear fuselage clearance during take-off

No.	Aircraft components	Clearance (m)	Remarks
1	Fuselage	0.2-1.2	
2	Rear fuselage	0.2-0.5	During take-off rotation
3	Wing	0.2-1.5	Includes flap clearance
4	Turbofan/turbojet engine	0.5-1.5	Inlet clearance
5	Stoke/fuel tank/pitot tube/antenna/probe	0.2-0.6	Tip clearance

The wheel base is defined as distance between nose gear and main gears. The load of nose gear must not carry over than %20 and must not carry less than %5. The load of main gear must not carry over than %95 and must not carry less than %80 so with these values for this design nose gear carry %10 main gears carry %90.  $W_0$  is taken with 1729kg payload which is the value is obtained as 19767kg from *Table 14* .

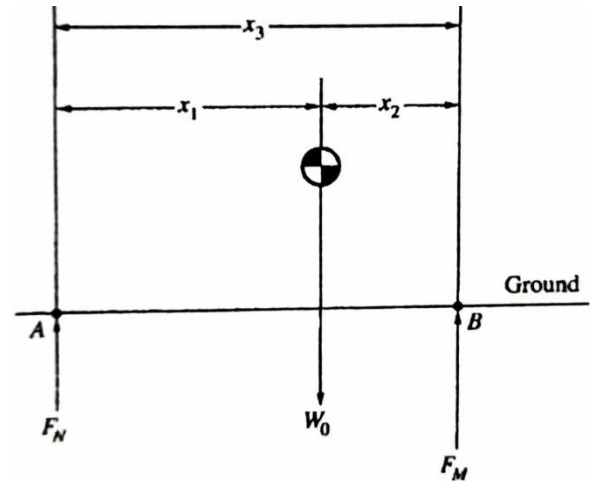


**Figure 26:**Wheel load geometry

The total forces are zero in the z direction;

$$\sum F_z = 0 \rightarrow F_n + F_m = W_0 \quad (63)$$

The total moments are zero with respect to B point;

$$\sum M_0 = 0 \rightarrow F_n * x_3 - W_0 * x_2 \quad (64)$$

So;

$$F_n = \frac{x_2}{x_3} W_0 = 1976.7 \text{ kg} \quad (65)$$

$$F_m = \frac{x_1}{x_3} W_0 = 8895.15 \text{ kg} \quad (66)$$

The location of nose gear is 3.36 meter from aircraft nose and main gear is 13.36 meter from aircraft nose.

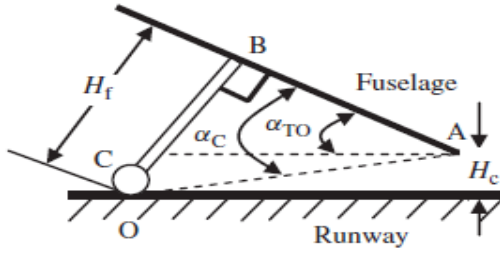


Figure 27 :Fuselage clearance during take-off rotation

The clearance angle ( $\alpha_C$ ) should be more than take-off (Tail-down) rotation angle ( $\alpha_{TO}$ ) and the take-off angle is about 10-15 degree. For this design take-off angle selected 12 degree and clearance angle selected 13 degree.

$$\alpha_C \geq \alpha_{TO}$$

$$H_f = \tan(\alpha_C) * AB \quad (67)$$

So, the distance between the fuselage and the ground is 1.567595 meter.

The distance of right main gear and left main gear is defined as wheel track (T) and overturn angle is defined as angle between vertical distance of center of gravity and intersection of main gears horizontal line, left or right main gear and center of gravity point line. The symbol of overturn angle is " $\Phi_{ot}$ ". The overturn angle should be larger than 25° degree. For this design overturn angle is selected as 30° degree.

$$\phi_{ot} \geq 25^\circ \quad (68)$$

The height of center of gravity is 2.89m from cg estimation.

$$Y_{ot} = \tan \phi_{ot} * H_{cg} \quad (69)$$

$$T \geq 2 * Y_{ot} \quad (70)$$

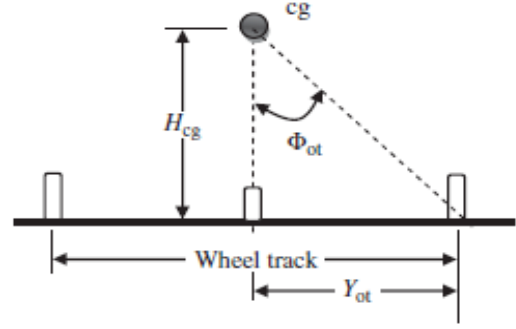


Figure 28:Overturn angle based on front view

The tip-back angle is the maximum aircraft nose-up attitude when the tail is touching the ground and the landing gear strut is fully extended. The tip-back angle always must be larger than the takeoff angle. So before, take of angle selected 12° degree. For this study tip-back angel selected 17° degree.

$$\alpha_{tb} \geq \alpha_{TO} + 5 \text{ deg} \quad (71)$$

The wheels are surrounded with a circular plastic object, this substance is named tire. Tire support the aircraft structure off the ground, reduces impact on landing and it help to drive of aircraft.

Table 34 : Empirical tire sizing

Main wheels diameter or width (in.) = $AW_W^B$			
Diameter		Width	
A	B	A	B
Jet	1,59	0,302	0,0980
fighter/trainer			0,467

$$W_W = \text{Wight on Wheel}$$

$$W_W = 0,9 * \frac{W_0}{2} = 0,9 * \frac{43578,78}{2} = 1961,45 \quad (72)$$

From the empirical tire sizing,

$$\text{Main gear diameter (D)} = \quad (73)$$

$$1,59 W_W^{0,302} = 31,4578 \text{ in}$$

$$\text{Main gear Width (W)} = 0.98 W_W^{0,967} = 9,9041 \text{ in} \quad (74)$$

Nose gear is 80% smaller than main gear so,

$$\text{Nose gear diameter (D)} = 0,8 * 31,4578 = 25,16624 \quad (75)$$



$$\text{Nose gear Width } (W) = 0,8 * 9,9041 \quad (76) \\ = 7,9233$$

The wheel diameters are taken from tire data table 11.2 from Raymer book page 235. The nose wheel diameter is 14 inch and the main gear wheel diameter is 16 inch.

## 11. Lift and Drag Calculations

### 11.1 Lift Curve Slope

Lift curve slope was obtained and drawn by using empirical formulas<sup>[1]</sup>. Between 0.1 Mach number and 0.8 Mach number subsonic lift curve slope was obtained by using Equations (77)(78) and (79).

$$C_{L\alpha} = \frac{2\pi AR}{2 + \sqrt{4 + \frac{AR^2 \beta^2}{\eta^2} (1 + \tan \Lambda_{\max,t}^2 / \beta^2)}} \frac{S_{\text{exposed}}}{S_{\text{ref}}} F \quad (77)$$

Where,

$$\beta^2 = 1 - M^2 \quad (78)$$

$$\eta = \frac{C_{l\alpha}}{2\pi/\beta} \quad (79)$$

$\Lambda_{\max,t}$  is the sweep of the wing at the thickest chord location and  $\eta$  represents the airfoil efficiency. Also,  $F$  is the fuselage lift factor which is shown in Eq. (80).

$$F = 1.07(1 + d/b)^2 \quad (80)$$

where  $d$  is the diameter of the fuselage which is selected as 1.95m.

**Table 35:** Parameters for  $CL\alpha$

Parameters	Values
$\tan \Lambda_{\max,t}$	0.699
$F$	1.21
$S_{\text{exposed}}/S_{\text{ref}}$	0.87

Transonic region Mach number range was determined by Eq. (81) and Mach critical number which was calculated as 0.89 in study-3 and it is determined in the range between 0.9M and 1.3M. In addition, sweep angle at leading edge is taken 44.42 degree. Lift curve slope values are determined according to Figure 29.

$$M > 1/\cos \Lambda_{LE} \quad (81)$$

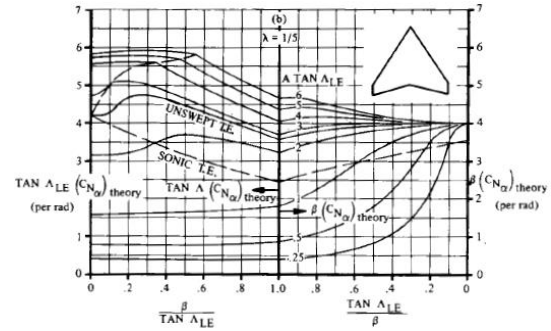


**Figure 29:** Normal Force Curve Slope for Supersonic Wings

Figure 29 used according to result of Eq. (81). If the results smaller than 1 left side of the figure and if the result was bigger than 1 the right side of the chart must be used. According to calculation left side was appropriate. Then, appropriate line was selected with the calculation of the  $AR$  times the tangent of the leading-edge sweep, and the vertical-axis values read. Required interpolations were done. Finally, lift curve slope was calculated for supersonic regime by using Eq. (82) Lift curve slope and graph were obtained.

$$C_{l\alpha} = 4/\beta \quad (82)$$

**Table 36:**  $CL\alpha$  vs. Mach Number

Mach Number	$C_{L\alpha}$
0.1	3.028572
0.2	3.050000
0.3	3.098102
0.4	3.163517
0.5	3.254837
0.6	3.379495
0.7	3.549987
0.8	3.788776
0.9	5.153291
1.0	5.469631
1.1	5.051245
1.2	4.571632
1.3	4.330021
1.4	4.082483

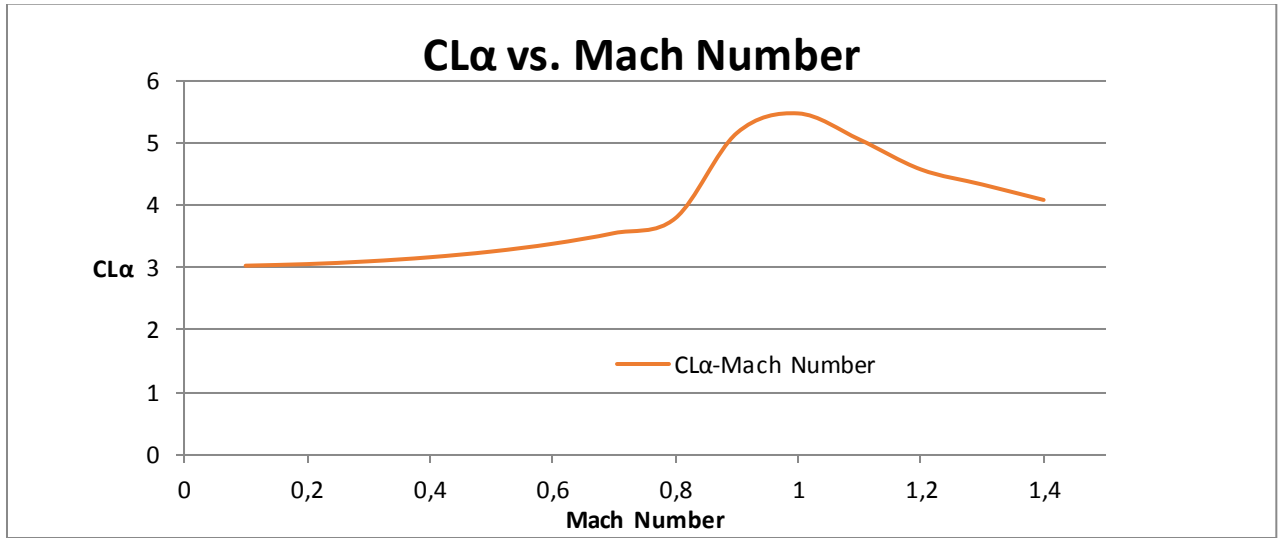


Figure 30:CLα vs. Mach Number Graph

### 11.2 Maximum Lift

Maximum lift of clean wing means that maximum lift of wing without high lift devices. To calculate lift coefficient of the wing firstly aspect ratio status of the wing defined with a formula that is given in the Eq. (83)<sup>[35]</sup>.

$$\text{Low AR if : } AR \leq \frac{3}{(C_1 + 1)(\cos \Lambda_{LE})} \quad (83)$$

where  $C_1$  is obtained from the Figure 31 as 0.5. Condition which is defined from the Eq. (83) is not satisfied so the status of wing with respect to aspect ratio is high aspect ratio. Lift coefficient of high aspect ratio wing calculated by the Eq (84).

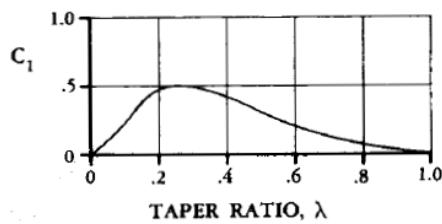


Figure 31:Taper Ratio Correction Factor for Low AR Wing

$$C_{L_{\max}} = C_{l_{\max}} \frac{C_{L_{\max}}}{C_{l_{\max}}} + \Delta C_{L_{\max}} \quad (84)$$

$C_{l_{\max}}$  is the airfoil maximum lift coefficient and that value was obtained as 1.168 from XFLR5. To calculate  $\frac{C_{L_{\max}}}{C_{l_{\max}}}$ , the leading edge sharpness parameter  $\Delta Y$  was calculated which is given in the Eq. (85) and according to the Figure 32 the value of that parameter was obtained.

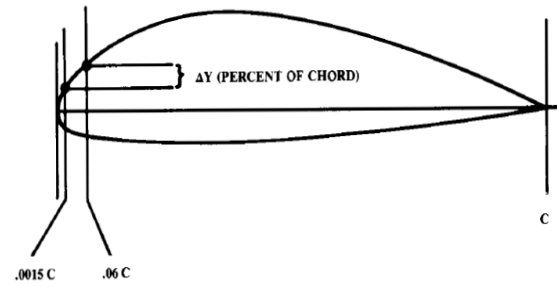
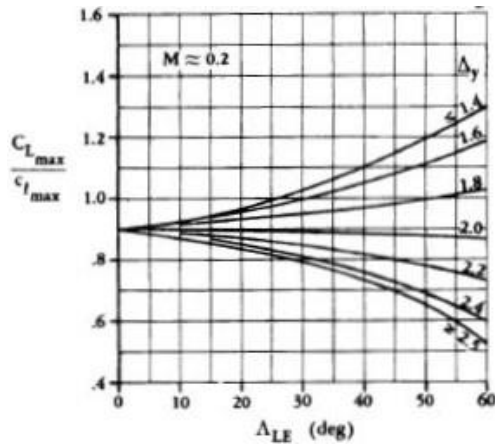


Figure 32 : Airfoil Leading Edge Sharpness Parameter

$$\Delta Y = 21.3(t/c) \quad (85)$$

$\Delta Y$  value was obtained as 1.704 from the Eq. (85).



**Figure 33 : Subsonic Maximum Lift of High AR Wing**

Then,  $\Delta C_{L_{max}}$  is the correction factor that is determined by using the Figure 34.

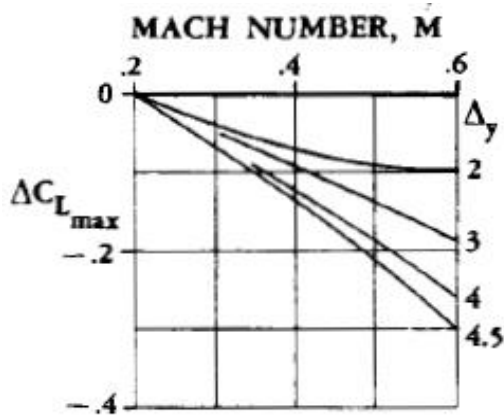


**Figure 34: Mach Number Correction for Subsonic Maximum Lift of High AR Wing**

**Table 37: Mach Number vs.  $C_{L_{max}}$**

Mach Number	$C_{L_{max}}$
0.2	1,71
0.5	1,65

Usable Lift coefficient is the lift coefficient of aircraft when it performs on cruise at sea level. Usable lift coefficient is calculated with the Eq. (86).

$$C_L = \frac{2W}{\rho M^2 a^2 S} \quad (86)$$

**Table 38: Usable  $CL$  vs Mach Number**

Mach Number	CL
0,2	1,405747
0,3	0,624776
0,4	0,351437
0,5	0,22492
0,6	0,156194
0,7	0,114755
0,8	0,087859
0,9	0,06942
1	0,05623
1,1	0,046471
1,2	0,039049
1,3	0,033272
1,4	0,028689

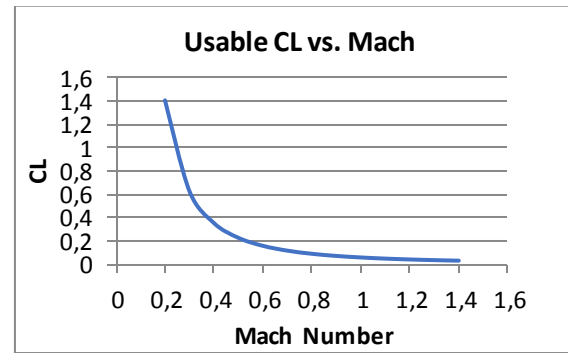


**Figure 35: CL vs Mach Number**

### 11.3 Maximum Lift with High Lift Devices

High lift devices are used to increase lift coefficient and stall angle of the wing. As high lift devices plain flap was selected for trailing edge flap to increase lift coefficient. Also, leading edge flap was used to increased stall angle and lift coefficient of the wing. Lift increment was calculated by the Eq. (87).

$$\Delta C_{L_{max}} = \Delta C_{L_{max}} \frac{S_{flapped}}{S_{ref}} \cos \Lambda_{HL} \quad (87)$$

Both leading and trailing edge flaps was designed cover the 90% of the wing span. In addition, hinge location was calculated with the Eq. (88).

$$\tan \Lambda_{LE} = \tan \Lambda_{HL} + \frac{4}{AR} X_{HL} \frac{1 - \lambda}{1 + \lambda} \quad (88)$$

Where  $X_{HL}$  is the hinge line location which is determined according to spar location.

**Table 39: High Lift Devices Values**

Plain Flap	Value
$Cl_{max}$	0.9
Hinge Line Location	0.9c
Hinge Line Angle	22.71°
$S_{flapped}/S_{ref}$	0.77
$\Delta CL_{max}$	0.51
Leading Edge Flap	
$Cl_{max}$	0.3
Hinge Line Location	0.1c
Hinge Line Angle	42.29°
$S_{flapped}/S_{ref}$	0.77
$\Delta CL_{max}$	0.16

**Table 40 : Lift Coefficient with High Lift Devices**

Mach Number	$CL_{max}$
0.2	2,38
0.5	2,33

## 11.4 Mach Divergence

The drag Mach divergence number ( $M_{DD}$ ) is critical parameter for the performance calculations. This value designates the end of subsonic the beginning of the transonic and supersonic region. It's the region where shocks start to be observed on the wing. Divergence Mach number could be calculated from the below the Eq. (89).

$$M_{DD} = M_{DD,L=0} LF_{DD} - 0.05 C_{L,design} \quad (89)$$

where  $M_{DD,L=0}$  is found from the Figure 36.

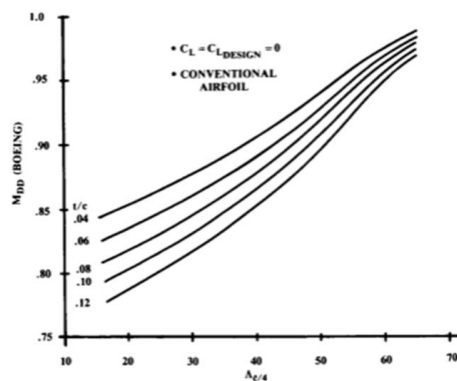


**Figure 36 : Wing drag divergence Mach number.**

The sweep angle in the previous studies was calculated as 44.4° at c/4 and by using the graph above the  $M_{DD,L=0}$  was calculated. The  $LF_{DD}$  value was calculated by using the graph below in the Figure 37.

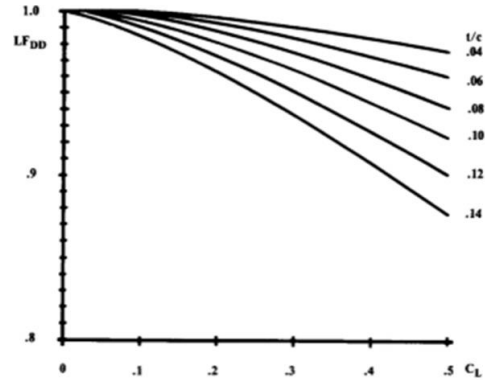


**Figure 37 : Lift Adjustment for drag divergence.**

As a result of the operations, the drag divergence Mach number for the wing was calculated as 0.7983. The drag divergence number calculations must be applied in same time on the fuselage. The  $M_{DD}$  on the fuselage was calculated according to the graph in the Figure 38.  $L_n$  is the length from the nose of the aircraft which the fuselage cross section becomes constant and  $d$  is the diameter of the equivalent diameter of the fuselage. This fraction was calculated as 12.31 where the  $M_{DD}$  for fuselage is equal to 0.93.

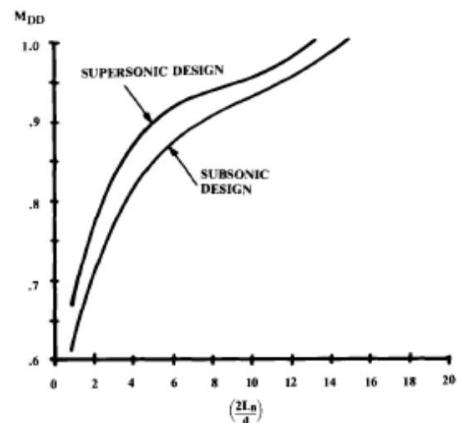


**Figure 38: Drag divergence estimation for the fuselage.**

The lower Mach number was selected because the transonic drag rise firstly will occur on the wing.

### 11.5 Parasite (Zero-Lift) Drag

There are two methods to predict parasite drag ( $C_{D_0}$ ). The first method is the most general one where in equation below ( $C_{f_e}$ ) skin friction coefficient, ( $S_{wet}$ ) wetted area of the airframe and ( $S_{ref}$ ) reference area of the wing.

$$C_{D_0} = C_{f_e} \frac{S_{wet}}{S_{ref}} \quad (90)$$

In the component build up method, the ( $C_{f_e}$ ) skin friction coefficient, (FF) form factor, (Q) interference factor, ( $S_{wet}$ ) wetted area and ( $S_{ref}$ ) reference area are the main parameters of the parasite drag calculation. The parasite drag of each component is calculated and the sum of all the components gives the parasite drag at subsonic regime. The subsonic parasite drag is obtained from the Eq. (91).

$$(C_{D_0})_{subsonic} = A + C_{D_{misc}} + C_{D_{L\&P}} \quad (91)$$

where

$$A = \frac{\sum(C_{f_e} FF_c Q_c S_{wet_c})}{S_{ref}} \quad (92)$$

The sub c at each parameter stands for component.

$C_{D_{misc}}$  is miscellaneous drag component and  $C_{D_{L\&P}}$  is leakage and protuberances drag component.

For laminar flow, skin friction coefficient becomes the form in the Eq (93) and for turbulent flow skin friction coefficient becomes the form in the Eq (94).

$$C_f = 1.328/\sqrt{Re} \quad (93)$$

$$C_f = \frac{0.455}{(\log_{10}^{Re})^{2.58} (1 + 0.144M^2)^{0.65}} \quad (94)$$

where

$$Re = \rho VL/\mu \quad (95)$$

L is characteristic length for each component. The calculated Reynolds number with the Eq. (95) could be lower than the actual one due to

the surface roughness. Therefore, cut off Reynolds number ( $R_{cutoff}$ ) should be used. The cut off Reynolds number for subsonic flow is given with the Eq (96).

$$R_{cutoff} = 38.21(l/k)^{1.053} \quad (96)$$

The cut off Reynolds number for transonic and supersonic flow its calculated with the Eq.(97).

$$R_{cutoff} = 44.62(l/k)^{1.053} M^{1.16} \quad (97)$$

k is the skin roughness values are shown below in the Table 41. For the intended design smooth melded composite category was chosen.

**Table 41 : Skin roughness value**

Surface	k - (ft)
Camouflage paint on aluminium	$3.33 \times 10^{-5}$
Smooth paint	$2.08 \times 10^{-5}$
Production sheet metal	$1.33 \times 10^{-5}$
Polished sheet metal	$0.50 \times 10^{-5}$
Smooth melded composite	$0.17 \times 10^{-5}$

The form factor in subsonic flows for wing, tail, strut and pylon could be calculated with using the Equations (98) and (99).

$$FF = B[1.34M^{0.18}(\cos \Lambda_m)^{0.28}] \quad (98)$$

where

$$B = \left[ 1 + \frac{0.6}{(x/c)_m} \left( \frac{t}{c} \right) + 100 \left( \frac{t}{c} \right)^4 \right] \quad (99)$$

$(x/c)_m$  is the maximum thickness location over the airfoil.  $\left( \frac{t}{c} \right)$  is the thickness of the airfoil.  $\Lambda_m$  is sweep angle at maximum thickness line of the airfoil.

Form factor for fuselage and smooth canopy could be calculated with the Eq. (100).

$$FF = \left( 1 + \frac{60}{f^3} + \frac{f}{400} \right) \quad (100)$$

where

$$f = \frac{l}{d} = \frac{l}{\sqrt{(4/\pi)A_{max}}} \quad (101)$$

d is the diameter of the fuselage and l is the length of the fuselage.  $A_{max}$  is the cross-section area of the fuselage.

The interference factor (Q) does has a specific equation. The values generally were selected depending the geometry of the airframe. The values of interference factor (Q) is shown below in *Table 42*.

**Table 42 :Interference Factor**

Component	Q
Nacelle/External stores mounted on wing or fuselage	1.5
Nacelle/External stores mounted less than one diameter away	1.3
Nacelle/External stores mounted beyond one diameter away	1.0
Wing Mounted Missiles	1.25
High wing/Mid wing/Well filleted low wing	1.0
Unfilled low wing	1.1–1.4
Fuselage	1.0
Tail	1.03

For this design the interference factor (Q) was taken as 1.0 for all of the components.

Miscellaneous drag calculation is done by summing 0.2 because machine gun ports add a D/q of about 0.2ft<sup>2</sup> per gun. By dividing this summation by reference area, the miscellaneous drag coefficient is obtained. The supersonic parasite drag could be expressed with the *Eq. (102)*.

$$(C_{D_0})_{\text{supersonic}} = (C_{D_0})_{\text{subsonic}} + C_{D_{\text{misc}}} + C_{D_W} \quad (102)$$

During the supersonic flight the new component of the drag coefficient is wave drag due to the shock waves. The wave drag in supersonic flight is greater than summation of all the other drags. An ideal volume distribution is obtained the Sears Haack body. A Sears-Haack body has a wave drag as in the *Eq. (103)*.

$$\left(\frac{D}{q}\right)_{\text{Sears-Haack}} = \frac{9\pi}{2} \left(\frac{A_{\text{max}}}{1}\right)^2 \quad (103)$$

For preliminary wave drag analysis, when at Mach is greater equal to 1.2 or greater than

1.2, a correlation to Sears-Haack body wave drag is represented in the *Eq. (104)*.

$$\left(\frac{D}{q}\right)_{\text{wave}} = E_{WD}[P] \left(\frac{D}{q}\right)_{\text{Sears-Haack}} \quad (104)$$

where

$$P = 1 - 0.386(M - 1.2)^{0.57} \quad (105)$$

and

$$P = \left(1 - \frac{\pi \Lambda_{LE}^{0.77}}{100}\right) \quad (106)$$

$E_{WD}$  is wave drag efficiency this number varies for different aircraft and it depending on volume distribution of the aircraft. This value is shown in more detail in the *Table 43*.

**Table 43: Wave Drag Efficiency**

Aircraft Type	$E_{WD}$
Smooth Blended/Delta wing	1.2
Supersonic Fighter/Bomber	1.4-2
Supersonic bumpy volume distribution	2-3

Transonic region is not able to be calculated by using formulation. Because of that reason, drag values corresponding to Mach number are used by estimating from the *Figure 39*.

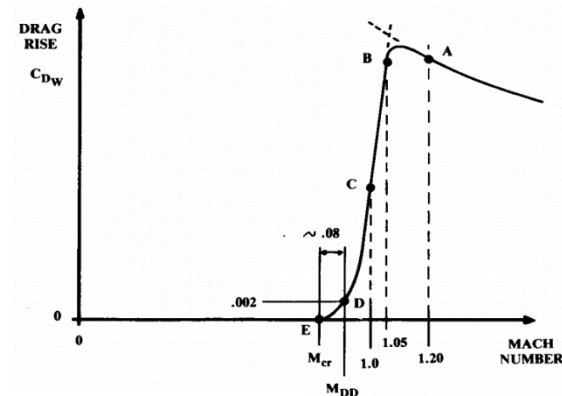


**Figure 39: Transonic drag rise estimation.**

At the end of the calculations the graph should look like the *Figure 40*. The obtained parasite drag values which varies depends on Mach number shown under the Result title in the *Table 49*.

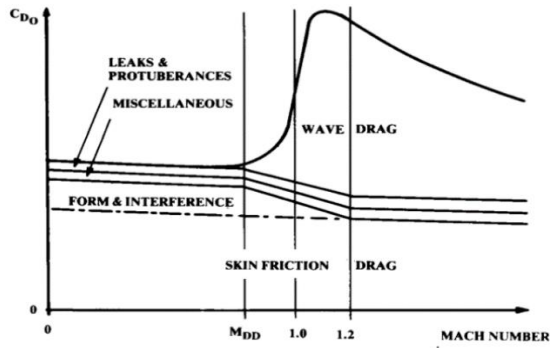


**Figure 40:** Complete parasite drag vs Mach number.

### 11.6 Induced Drag Factor

Induced drag ( $C_{Di}$ ) is the drag due to lift. The component could present as shown in the Eq. (107).

$$C_{Di} = KC_L^2 \cong \alpha C_L \quad (107)$$

$K$  is the induced drag factor.

Leading edge suction method, is a semi empirical method which allows the variation of ( $K$ ) with lift coefficient and Mach number, since the Oswald span efficiency method ignores the variation of ( $K$ ) with lift coefficient and for most supersonic aircrafts it gives a poor approximation. Figure X illustrates the concept of leading-edge suction. The term ( $S$ ) presents the suction force and ( $N$ ) the normal force.

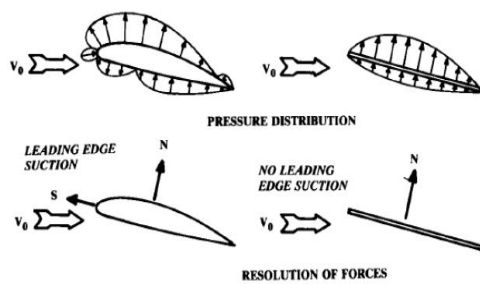


**Figure 41:** Leading edge suction definition.

In 3D wing is considered to have 100% leading edge suction where the Oswald efficiency factor ( $e$ ) becomes equal to 1.0. So, the induced drag coefficient could be found from the Eq. (108).

$$K_{100} = \frac{1}{\pi e AR} \quad (108)$$

For the worst case of zero leading edge suction, so the drag due to lift factor ( $K$ ) becomes the inverse of the slope of the lift curve slope and is shown below in the Eq. (109)

$$K_0 = \frac{1}{C_{L\alpha}} \quad (109)$$

The  $K_0$  and  $K_{100}$  are equal to each other at Mach number is equal to inverse of sine of  $90^\circ$  minus the leading-edge sweep angle. At sweep angle is  $44.4^\circ$  and the  $K_0$  and  $K_{100}$  are equal each other  $M=1.3996$ . The  $K_0$  and  $K_{100}$  induced drag factors graph is shown below in the Figure 42.

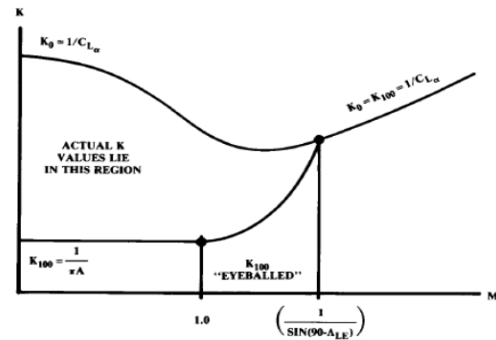


**Figure 42:**  $K_0$  and  $K_{100}$  factors vs Mach number.

In real the wings operate somewhere between 100% and 0% leading edge suction. The percentage of leading edge suction a wing attains is called ( $S$ ) which is different from the leading-edge suction force ( $S$ ). During the subsonic cruise, a wing will have ( $S$ ) about 0.85 – 0.95. During the design the value was taken as 0.9 and the wing supersonic fighter mat have an ( $S$ ) approaching to zero.

The actual ( $K$ ) is calculated as a weighted average of the 100% and 0%. Therefore, it was calculated with Eq.(110).

$$K = SK_{100} + (1 - S)K_0 \quad (110)$$

The results of the induced drag factors are shown below in the Figure 43, Figure 44 and Figure 45.

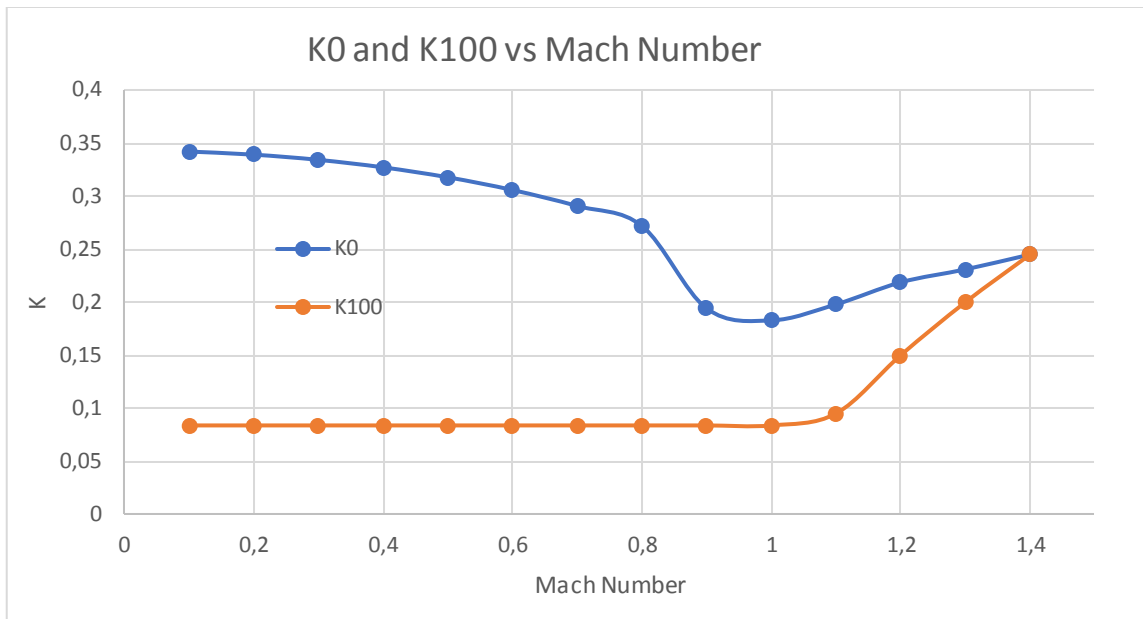


**Figure 43:** K100 and K<sub>0</sub> vs Mach number.

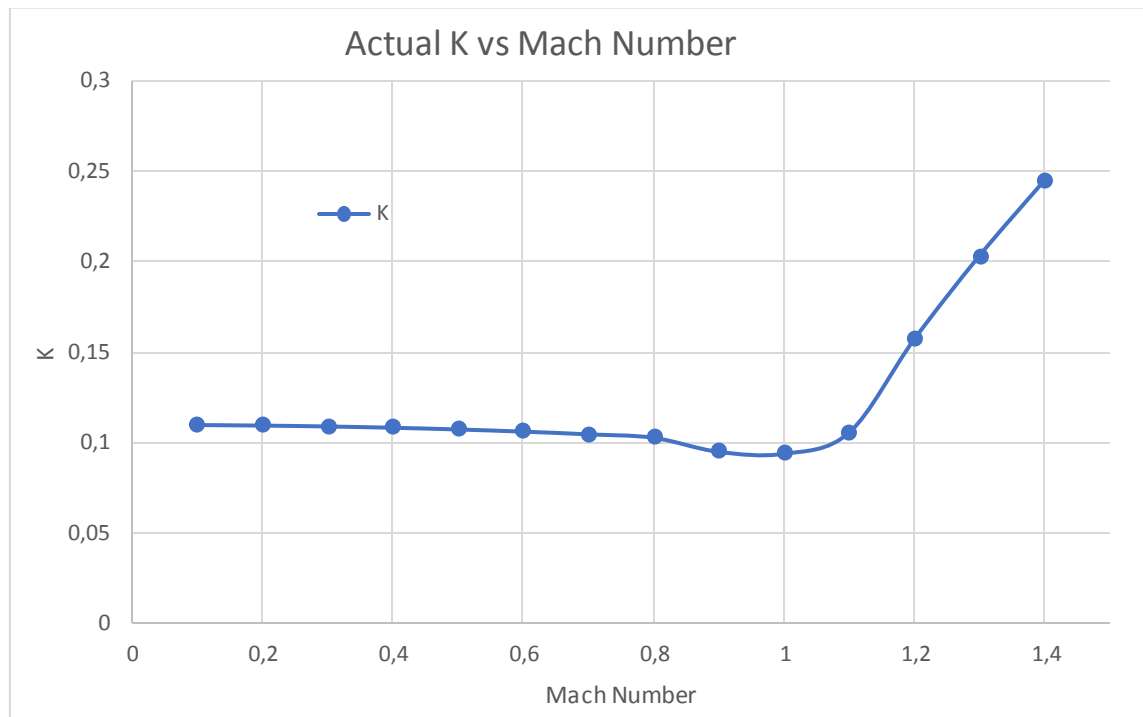


**Figure 44:** Actual K vs Mach number.



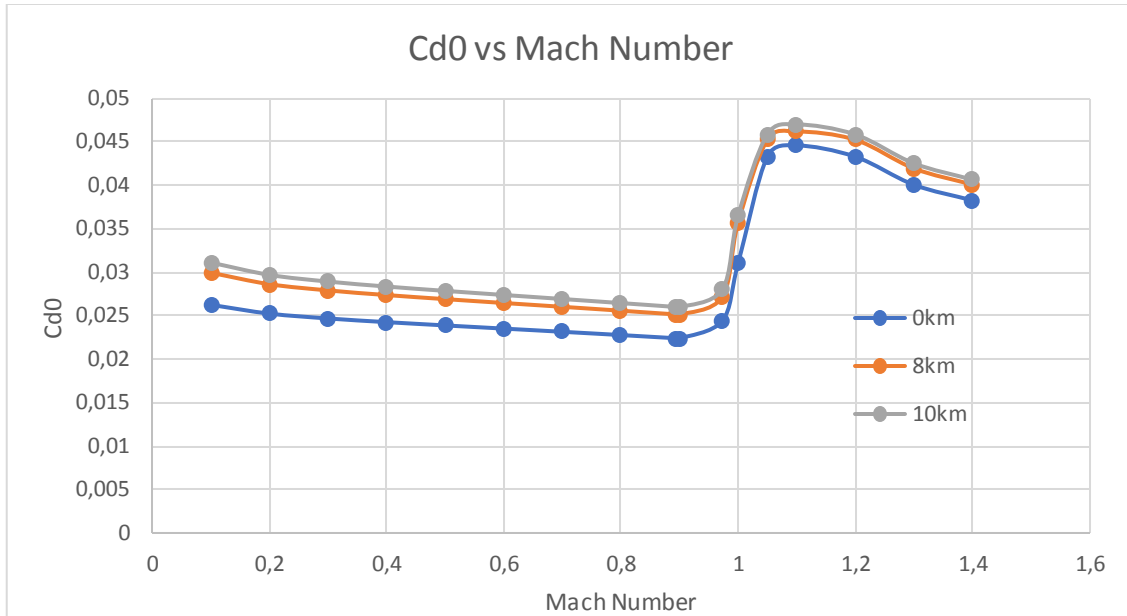


Figure 45: Cd0 vs Mach number graph.

## 12. Steady Flight Aircraft Performance Analysis

### 12.1 Service & Absolute Ceiling

As it is stated in the requirements, the service ceiling of the fighter aircraft is the necessity to find for this particular part of the study. The term is directly related to the maximum rate of climb value, meaning that if the rate of climb value becomes 0 m/s, that altitude is called absolute ceiling, however if the rate of climb value hits 0.5 m/s, this time the altitude is

called service ceiling. The sea level condition was utilized in the calculations of the service ceiling and absolute ceiling. The relation of the density and thrust available according to altitude is used that is shown the *Eq. (111)*. Also,  $m$  is depending on the engine but generally  $m \cong 1$  so it is taken as 1. Absolute ceiling is found as 21885 meters and service ceiling is found as 21792 meters.

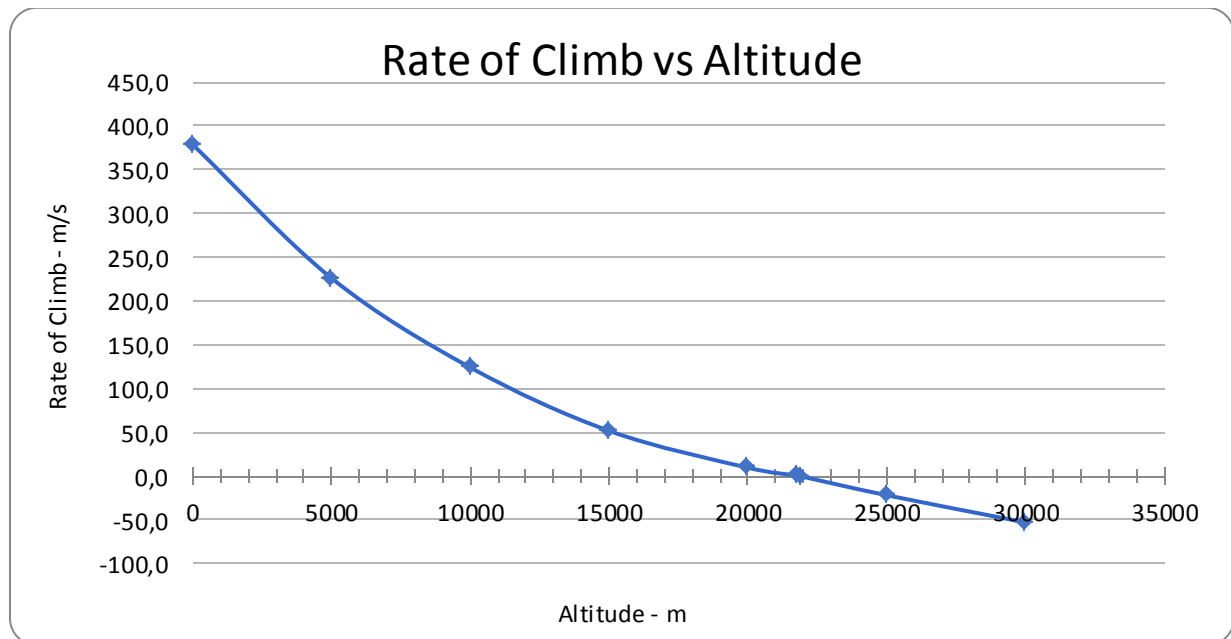


Figure 46: Rate of Climb VS Altitud

$$\left(\frac{T}{T_0}\right) = \left(\frac{\rho}{\rho_0}\right)^m \quad (111)$$

## 12.2 Rate of Climb

Rate of climb is the vertical component of the velocity of the aircraft. As it is stated in the requirements, rate of climb is calculated at sea level conditions, engine gives maximum thrust so rate of climb become maximum. Rate of climb maximum is calculated with the Eq. (112) that is stated in the Raymer's book which is shown below and according to total velocity of aircraft is also given below the Eq. (113).

$$V_v = \text{ROC}_{\max} = v \left( \frac{T-D}{W} \right) = v \left( \frac{T}{W} - \frac{\rho V^3 C_{D0}}{2 \left( \frac{W}{S} \right)} - \frac{2K}{\rho V} \left( \frac{W}{S} \right) \right) \quad (112)$$

$$V = \sqrt{\frac{\frac{W}{S}}{\rho V^3 C_{D0}} \left[ \frac{T}{W} + \sqrt{\left( \frac{T}{W} \right)^2 + 12 C_{D0} K} \right]} \quad (113)$$

## 12.3 Range

The range is the total distance a plane travels with a fuel load. Range is described by R. For calculate the range some weight variables are necessary. These weights are gross weight ( $W_0$ ), weight of fuel ( $W_f$ ) and weight of the airplane when the fuel tanks are empty ( $W_1$ ). The gross weight ( $W_0$ ) of the airplane including every possible load these are ranked as full fuel load, payload, crew and structure. At any instant during the flight, the weight of the airplane ( $W$ ) is found summation of the weight of the airplane when the fuel tanks are empty situation with weight of fuel. The range is closely linked to engine performance with specific fuel consumption. For the suitable jet-propelled airplanes engine type, the specific fuel consumption has been obtained as 0,0002 1/s. The main important component of power is specific fuel consumption. The specific fuel consumption is described by  $c_t$ . For maximum range for the

jet related with  $V_\infty (L/D)$ . For the steady level flight,

$$L = W = \frac{1}{2} \rho_\infty V_\infty^2 S C_L \quad (114)$$

Or

$$V_\infty = \sqrt{\frac{2W}{\rho_\infty S C_L}} \quad (115)$$

Thus,

$$V_\infty (L/D) = \sqrt{\frac{2W}{\rho_\infty S C_L}} \frac{C_L}{C_D} = \sqrt{\frac{2W}{\rho_\infty S}} \frac{C_L^{1/2}}{C_D} \quad (116)$$

The important point is the  $V_\infty (L/D)$  maximum when  $C_L^{1/2}/C_D$  is maximum. Then, the integration of (W) in previous equation and substituting in general range equation and that found like in the Eq. (117).

$$R = \int_{W_1}^{W_0} \frac{1}{c_t} \sqrt{\frac{2W}{\rho_\infty S}} \frac{C_L^{1/2}}{C_D} \frac{dW}{W} \quad (117)$$

Assuming  $c_t, \rho_\infty, S$  and  $C_L^{1/2}/C_D$  are constant and the general equation is like in the Eq. (118).

$$R = \frac{1}{c_t} \sqrt{\frac{2}{\rho_\infty S}} \frac{C_L^{1/2}}{C_D} (W_0^{1/2} - W_1^{1/2}) \quad (118)$$

For the maximum range according to general formula, the jet fly maximum  $C_L^{1/2}/C_D$ , have the lowest possible thrust specific fuel consumption, fly at high altitude, where  $\rho_\infty$  is small and carry a lot of fuel. The  $C_L^{1/2}/C_D$  equation follow that the theoretical maximum range for a jet airplane is obtained by flying at the velocity where the relation between zero lift drag and drag due to lift becomes like in the Eq. (119).

$$C_{D,0} = 3KC_L^2 \quad (119)$$

The velocity become like in the Eq. (120).

$$V_{(C_L^{1/2}/C_D)_{\max}} = \left( \frac{2}{\rho_\infty} \sqrt{\frac{3K}{C_{D,0}}} \frac{W}{S} \right)^{1/2} \quad (120)$$

The  $C_L^{1/2}/C_D$  value become like in the Eq. (121).

$$\left(\frac{C_L^{1/2}}{C_D}\right)_{\max} = \frac{3}{4} \left(\frac{1}{3KC_{D,0}^3}\right)^{1/4} \quad (121)$$

For this design project range calculated at sea level altitude with full payload and without payload so for this project payloads are 4L-Umtaş, 2-MK83, 3-Bozdoğan and ammo. Their total weight is 3811.7 lb.

#### 12.4 Endurance

Endurance is the time during which a plane can remain in a single fuel load in the air. Maximum endurance for a jet-propelled driven airplane corresponds to flying at the maximum L/D ratio, having the lowest possible thrust specific fuel consumption and having the highest possible ratio of  $W_0$  to  $W_{13}$ . The maximum L/D ratio found like in the Eq. (122).

$$\left(\frac{L}{D}\right)_{\max} = \left(\frac{C_L}{C_D}\right)_{\max} = \sqrt{\frac{1}{4KC_{D,0}}} \quad (122)$$

The  $\left(\frac{L}{D}\right)_{\max}$  is found as 13.75371. The general endurance formula is like in the Eq. (123). With using the Eq (122) and Eq (123) the new form of equation become for maximum condition like in the Eq (124).

$$E = \frac{1}{c_t} \frac{L}{D} \ln \frac{W_0}{W_{13}} \quad (123)$$

For this design project endurance calculated at sea level altitude with full payload and without payload. Gross weight( $W_0$ ) is 43578,98 lb and ( $W_{13}$ ) is 27991,28 lb are found with payload.

$$E = \frac{1}{c_t} \frac{L}{D} \ln \frac{W_0}{W_{13}} = \frac{1}{c_t} \sqrt{\frac{1}{4KC_{D,0}}} \ln \frac{W_0}{W_{13}} \quad (124)$$

For without payload gross weight( $W_0$ ) is 39767,28 lb and ( $W_{13}$ ) is 24179,58 with th endurance results are shown below in the Table 44.

**Table 44:** Range and Endurance with and without payload

	With payload	Without payload
<b>Range (km)</b>	2592,18	2746,63
<b>Endurance(hour)</b>	6.20	6.97

#### 12.5 Maximum Velocity

The maximum velocity is the highest speed of the aircraft which can reach. Maximum velocity directly related with thrust. In steady, level flight, the maximum velocity of the aircraft is determined by the high-speed intersection of the thrust required and thrust available curves. For flight at  $V_{\max}$ , the thrust available is at its maximum value is obtained in the Eq. (125).

$$T_R = (T_A)_{\max} \quad (125)$$

For this design calculated maximum speed with and without afterburner at sea level altitude with weight after dogfight, so for this design weight fraction after dogfight calculated 0,711 so weight is after dogfight ( $W_{\text{adf}}$ ) calculated like in the Eq. (126).

$$W_{\text{adf}} = W_0 * 0,71 = 27202.73\text{lb} \quad (126)$$

The maximum thrust ( $T_R$ ) for chosen engine is for afterburner 55078,19 and for dry thrust value is 30798,25. The maximum velocity formula is given in the Eq. (127).

$$V_{\max} = \left[ \frac{\{T_R/W\} * (W/S) + (W/S) \sqrt{\{T_R/W\}^2 - 4KC_{D,0}}}{\rho_{\infty} C_{D,0}} \right]^{1/2} \quad (127)$$

The maximum velocity proportional with  $T_R/W$  and  $W/S$  other vice inversely proportional with  $C_{D,0}$  and  $K$ . The results are shown below in the Table 45.

**Table 45:** Maximum Velocity with and without afterburner

	Velocity(m/s)	Mach Number
<b>Maximum Velocity (with AB)</b>	428,25	1,258
<b>Maximum Velocity (Dry)</b>	573,07	1,68

#### 12.6 Stall Speed

The stall velocity of an airplane is one of its most important performance characteristics. The take-off and landing speeds are slightly higher than  $V_{\text{stall}}$  because stall speed is the slowest speed that an aircraft can fly. From the Eq.(128) stall speed was obtained at sea level

is 117.81 and also obtained with high lift devices 108.67.

$$V_{stall} = \sqrt{\frac{2}{\rho_{\infty}} \frac{W}{S} \frac{1}{C_{L_{max}}}} \quad (128)$$

## 12.7 Take-off and Landing Distance

### 12.7.1 Calculation Ground Roll

$C_{L_{max}}$  value is obtained for 0.2 Mach .  $\mu_r$  was obtained from the Anderson book at Table 6.1<sup>[36]</sup> and it is dry concrete/ asphalt was 0.04 for brakes off. Calculating the takeoff static friction and dynamic friction effects calculated between asphalt friction and the wheels. Take off distance is obtained 278 meters and takeoff time is 9.44 s. Results are obtained from the Equations (129)(130) and(131) and shown in the Table 46.

**Table 46:** Take-off Results

Take-off Distance	Take-off Time
278 meters	9.44 s.

$$T - \text{static friction} = \frac{W}{g} \alpha \quad (129)$$

$$V_{LO} = 1.1V_{stall} \quad (130)$$

$$\frac{dV_{\infty}}{dt} = T - D - \mu_r(W - L) \quad (131)$$

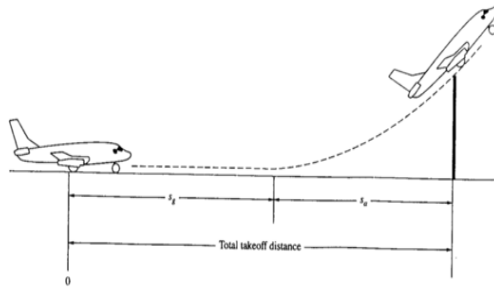


**Figure 47 :**Take-off configuration

**Table 47 :**Brake off and on friction coefficient

Surface	Brakes off	Brakes on
Dry concrete/asphalt	0.03-0.05	0.3--0.5
Wet concrete/asphalt	0.05	0.15-0.3
Icy concrete/asphalt	0.02	0.06-0.1
Hard turf	0.05	0.4
Finn dirt	0.04	0.3
Soft turf	0.07	0.2
Wet grass	0.08	0.2

## 12.8 Landing and Ground Roll Calculation

Calculating dynamic friction effects calculated between asphalt friction and the wheels. Landing approached distance is obtained 143.49 meters and flair distance 323.35 meter. Ground roll  $s_g$  is obtained 118.26 meter. Ground roll time is obtained 5.85 s. Results for landing gear are obtained from the Equations (132),(133),(134),(135),(136),(137),(138)(139) ,(140),(141),( 142) and shown in the Table 48.

**Table 48:** Landing Gear Results

Landing Approached	Flair Distance	Ground Roll $s_g$	Ground Roll Time
143.49 meters	323.35 meters	118.26 meters	5.85 s.

Calculating approach distance

$$L = W \cos \theta_{\alpha} \quad (132)$$

$$D = T + W \sin \theta_{\alpha} \quad (133)$$

$$\sin \theta_{\alpha} = \frac{1}{L/D} \frac{T}{W} \quad (134)$$

$$h_f = R(1 - \cos \theta_{\alpha}) \quad (135)$$

$$R = \frac{V_f}{0.2g} \quad (136)$$

$$V_a = 1.23V_{stall} \quad (137)$$

$$V_{TD} = 1.1V_{stall} \quad (138)$$

$$V_f = 1.15V_{stall} \quad (139)$$

Calculating of flare distance;

$$s_f = R \sin \theta_{\alpha} \quad (140)$$

$$s_a = (15.24 - h_f) / \tan \theta_a \quad (141)$$

Calculation of Ground Roll

$$m \frac{dV_\infty}{dt} = -T_{rev} - D - \mu_r(W - L) \quad (142)$$

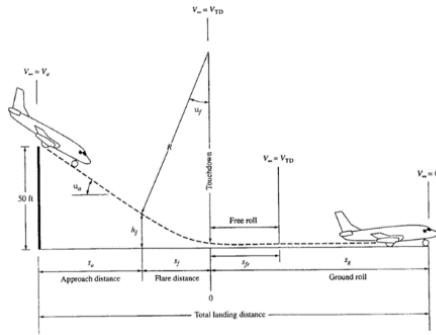


Figure 48: Landing configuration

### 13. Accelerated Flight Aircraft Performance Analysis

#### 13.1 V-n Diagram

The V-n diagram shows the aerodynamic and structural limitations for any aircraft. These diagrams are unique for every aircraft. It is a type of 'flight envelope' for the given aircraft. The V-n diagram for the designed aircraft. Stall region can also be seen on the figure. There is also  $V^*$  value which is called the corner velocity. The  $V^*$  corresponds to point B which shows that both  $C_L$  and  $n$  are at their highest possible values for an allowable flight. That means if the aircraft wants to fly at a higher value than  $V^*$ , it should fly at values less than  $(C_L)_{max}$  in the form of Eq. (143) shows the calculation of the velocity.  $V^*$  is obtained as 155.41 m/s

$$V = \sqrt{\frac{2n}{\rho_\infty C_L} \frac{W}{S}} \quad (143)$$

The maximum load factor was taken account as 8.5 which corresponds to the point B. If  $n$  is greater than the limit load factor it will occur a structural damage. But if  $n$  is greater than the ultimate load factor which is 1.5 times of maximum load factor, parts of the airplane will break. Diagram shown in the result part in the Figure 51.

### 14. Stability Analysis

Longitudinal static stability is an important parameter for static stability of aircraft. Static stability is the tendency of the aircraft to return to its trim condition after a nose up or nose down disturbance. To calculate longitudinal stability, neutral point and pitch stiffness derivative calculated by using the Eq. (144) and Eq. (145) respectively.<sup>[35]</sup>

$$\bar{X}_{np} = \frac{C_{L\alpha} \bar{X}_{acw} - C_{m\alpha fus} + \eta_h \frac{S_h}{S_w} C_{L\alpha h} \frac{\partial \alpha_h}{\partial \alpha} \bar{X}_{ach} + \frac{Fp_\alpha}{q S_w} \frac{\partial \alpha_p}{\partial \alpha} \bar{X}_p}{C_{L\alpha} + \eta_h \frac{S_h}{S_w} C_{L\alpha h} \frac{\partial \alpha_h}{\partial \alpha} + \frac{Fp_\alpha}{q S_w}} \quad (144)$$

$$C_{m\alpha} = -C_{L\alpha} (\bar{X}_{np} - \bar{X}_{cg}) \quad (145)$$

Most forward cg location was found at and the most rearward cg was found as 11.79m and 12.62m.  $C_{L\alpha h}$  was calculated by using XFLR5. For finding longitudinal stability downwash and up-wash angle was calculated. For subsonic regime, Eq (146)<sup>[39]</sup> was used and for supersonic regime Eq. was used. Tail angle of attack derivative calculated by the Eq. (147).  $\bar{X}_{acw}$ ,  $\bar{X}_{ach}$ , and  $\bar{X}_p$  taken as 7.92, 15, and 13.22 respectively.

$$\frac{\partial \epsilon}{\partial \alpha} = \frac{2C_{L\alpha}}{\pi AR} \quad (146)$$

$$\frac{\partial \epsilon}{\partial \alpha} = \frac{1.62 C_{L\alpha}}{\pi AR} \quad (147)$$

$$\frac{\partial \alpha_h}{\partial \alpha} = 1 - \frac{\partial \epsilon}{\partial \alpha} \quad (148)$$

To calculate up-wash angle was calculated as 0.5 with Figure 49.

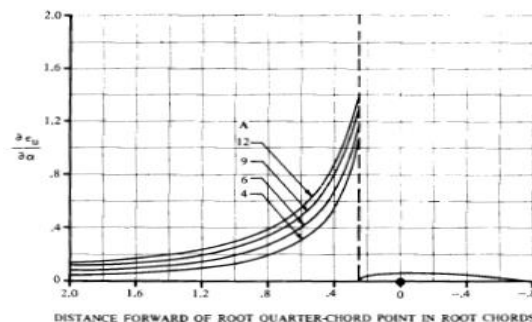


Figure 49: Upwash Estimation

Also, change in up-wash angle with respect to angle of attack was calculated by using Eq. (149) and it is found as 1.5.

$$\frac{\partial \alpha_u}{\partial \alpha} = 1 + \frac{\partial \epsilon_u}{\partial \alpha} \quad (149)$$

Fuselage pitching moment approximated with Eq. (150). Parameters in the Eq. (150) which are  $K_f$  is the empirical pitching moment factor,  $W_f$  is the width of the fuselage, and  $L_f$  is the length of fuselage.  $K_f$  is obtained as 0.02 from Figure 50. It is obtained as 11.6974.

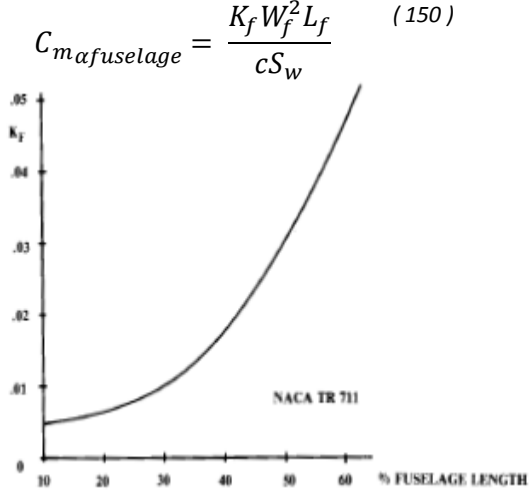


Figure 50: Position of  $\frac{1}{4}$  root chord

$F_p$  is the normal force due to the turning of the air<sup>[35]</sup>. It can be calculated from momentum consideration. Normal force with respect to angle of attack was calculated with Eq. (151). Also, mass flow rate was calculated with Eq. (152).  $F_{p_\alpha}$  is obtained as 255350 kgm/s<sup>2</sup> and  $\dot{m}$  obtained as 536.4520 kg/s.

$$F_{p_\alpha} = \dot{m}V \quad (151)$$

$$\dot{m} = \rho V A_{inlet} \quad (152)$$

In addition,  $\eta_h$  is the tail dynamic pressure ratio and it is accepted as 0.9<sup>[35]</sup>. Static margin is calculated with Eq. (153).

$$\text{Static Margin} = \bar{X}_{np} - \bar{X}_{cg} \quad (153)$$

Most forward and most rearward cg is calculated as shown in results parts in the

Table 50 and Table 51 respectively. Neutral point and pitch stiffness are obtained due to Mach number for forward and rearward cg location and shown in the results parts Figure 52, Figure 53 and Figure 54.

## 15. Cost Analysis

After all the calculations and the design of the aircraft the final step is the cost analysis. This part is important due to the consistency of the total cost and performance of the aircraft. there is also a fact and it says; how more aircraft produced the more manufacturer learns and the cheaper the next aircraft can be produced. this is known as the learning curve. Due to this effect, the cost comparisons are not meaningful between a new aircraft just entering the production and an old aircraft already produced hundred or thousand times. The cost difference between a new and a old aircraft is that the old aircrafts (which are produced for long times) has only a production cost, only includes the labour and material cost to manufacture the aircraft, including airframe, engines and avionics. But for a new designed aircraft, RDT&E has to be considered. This stands for research, development, test and evaluation, which includes all the technology research, design engineering, prototype fabrication, flight and ground testing, and evaluation for operational suitability. All these cost are directly estimated by DAPCA.

Making a cost estimation is mostly statistical. Cost data for a number of aircraft are analysed using curve-fit programs to prepare "cost estimating relationships" (CER). RAND Corporations, known as "DAPCA IV" has developed a set of CERs and modified the latest version of the development and procurement costs of the aircraft. this is called DAPCA model. It is not the best estimation for all types of aircrafts but reasonable for fighters bombers and transports. That is why this DAPCA model is a good cost estimation that can be used for the designed jet trainer aircraft.

(modified DAPCA IV cost model (cost in constant 1986 dollars))

$$\text{Eng hours} = 4.86 W_e^{0.777} V^{0.894} Q^{0.163} = H_E \quad (154)$$

$$\text{Tooling hours} = 5.99 W_e^{0.777} V^{0.696} Q^{0.263} = H_T \quad (155)$$

$$\text{MFG hours} = 7.37 W_e^{0.82} V^{0.484} Q^{0.641} = H_M \quad (156)$$

$$\text{QC hours} = 0.133 (\text{mfg hours}) = H_Q \quad (157)$$

$$\text{Devel support cost} = 45.42W_e^{0.630}V^{1.3} = C_D \quad (158)$$

$$\text{Flt test cost} = 1234.03W_e^{0.325}V^{0.822}FTA^{1.21} = C_F \quad (159)$$

$$\text{Mfg materials cost} = 11.0W_e^{0.921}V^{0.621}I^{0.799} = C_M \quad (160)$$

$$\text{Eng production cost} = 1548[0.043T_{max} + 243.25M_{max} + 0.969T_{turbine inlet} - 2228] = C_{eng} \quad (161)$$

$$\text{RDT\&E + flyaway} = H_E R_E + H_T R_T + H_M R_M + H_Q R_Q + C_D + C_F + C_M + C_{eng} N_{eng} + C_{avionics} \quad (162)$$

## RESULTS

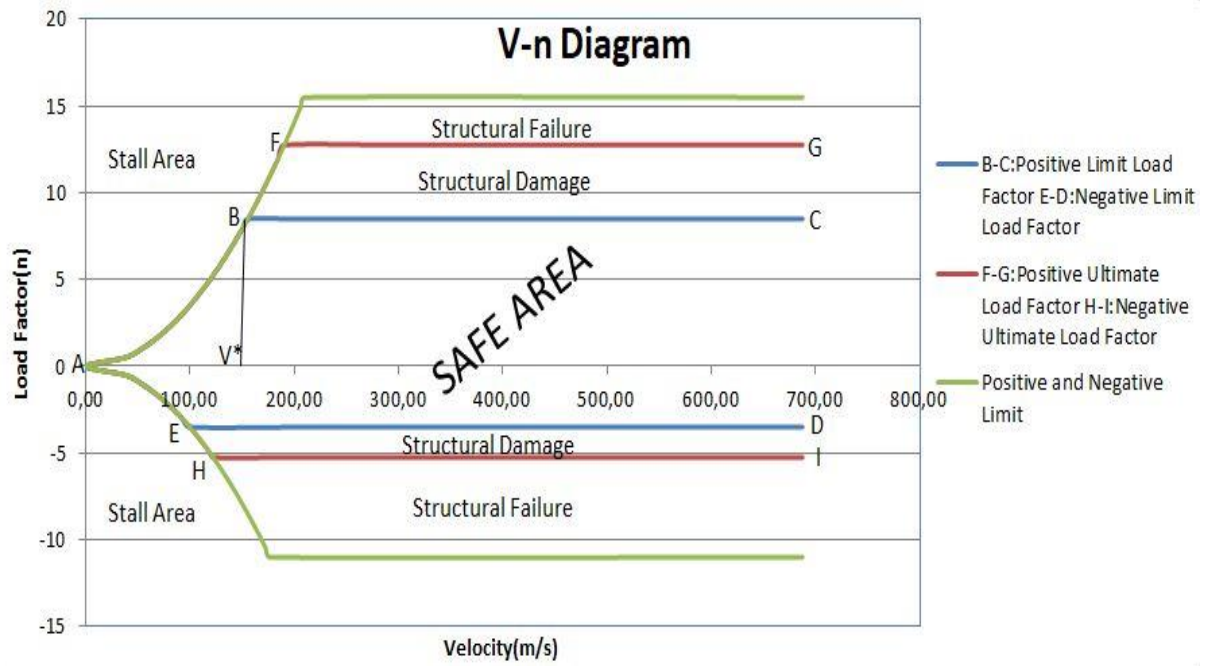


Figure 51: V-n Diagram

Table 49: CD0 data for different altitudes.

	Sea Level	8km Altitude	10km Altitude
Mach	Cd0	Cd0	Cd0
0.1	0.026258	0.029943	0.031112
0.2	0.025249	0.028633	0.029701
0.3	0.024696	0.02792	0.028936
0.4	0.024274	0.027386	0.028365
0.5	0.023897	0.026919	0.027868
0.6	0.023532	0.026475	0.027398
0.7	0.023164	0.026034	0.026934
0.8	0.022787	0.025589	0.026465
0.9	0.022399	0.025133	0.025988
1	0.030998	0.035667	0.036501
1.1	0.044586	0.04619	0.047003
1.2	0.043297	0.045243	0.04585
1.3	0.040073	0.041952	0.042538
1.4	0.038275	0.040089	0.040655

**Table 50: Most Forward Cg Location**

Part	Mass (kg)	X (m)	Xm (kgm)	Z (m)	Zm (kgm)
Horizontal Tail	197,32	17,882	3528,47624	-0,4	-78,928
Vertical Tail	55	17,6	968	0,55	30,25
Engine	3500	16,22	56770	0	0
Fuselage	4177	8,95	37384,15	0	0
Crew	170	3,5	595	0,15	25,5
4L-Umtaş	150	12	1800	-0,48	-72
2Gökdoğan	170	9,9	1683	-0,48	-81,6
1Gökdoğan	85	11,5	977,5	-1,43	-121,55
2Mk-83	908	10	9080	-0,178	-161,624
Ammo	200	2	400	-0,95	-190
Gun	100	2	200	-1,03	-103
Main Landging Gear	918,83	13,36	12275,5688	-2,89	-2655,419
Nose Landging Gear	334	3,36	1122,24	-2,89	-965,26
Wing	1581	12,08	19098,48	-0,4	-632,4
Fuel Tank	7070,4626	12,1	85552,59734	-0,4	-2828,185
Total	19616,613		231435,0124		-5006,031

**Table 51 : Most Rearward Cg Location**

Part	Mass (kg)	X (m)	Xm (kgm)	Z (m)	Zm (kgm)
Horizontal Tail	197,32	17,882	3528,4762	-0,4	-78,928
Vertical Tail	55	17,6	968	0,55	30,25
Engine	3500	16,22	56770	0	0
Fuselage	4177	8,95	37384,15	0	0
Crew	170	3,5	595	0,15	25,5
4L-Umtaş	150	14	2100	-0,48	-72
2Gökdoğan	170	10,9	1853	-0,48	-81,6
1Gökdoğan	85	12,5	1062,5	-1,43	-121,55
2L-Umtas	75	11	825	-0,178	-13,35
Ammo	200	2	400	-0,95	-190
Gun	100	2	200	-1,03	-103
Main Landging Gear	918,83	13,36	12275,569	-2,89	-2655,419
Nose Landging Gear	334	3,36	1122,24	-2,89	-965,26
Wing	1581	12,08	19098,48	-0,4	-632,4



<b>FuelTank</b>	7000	14	98000	-0,4	-2800
<b>Total</b>	18713,15		236182,42	-	4857,757

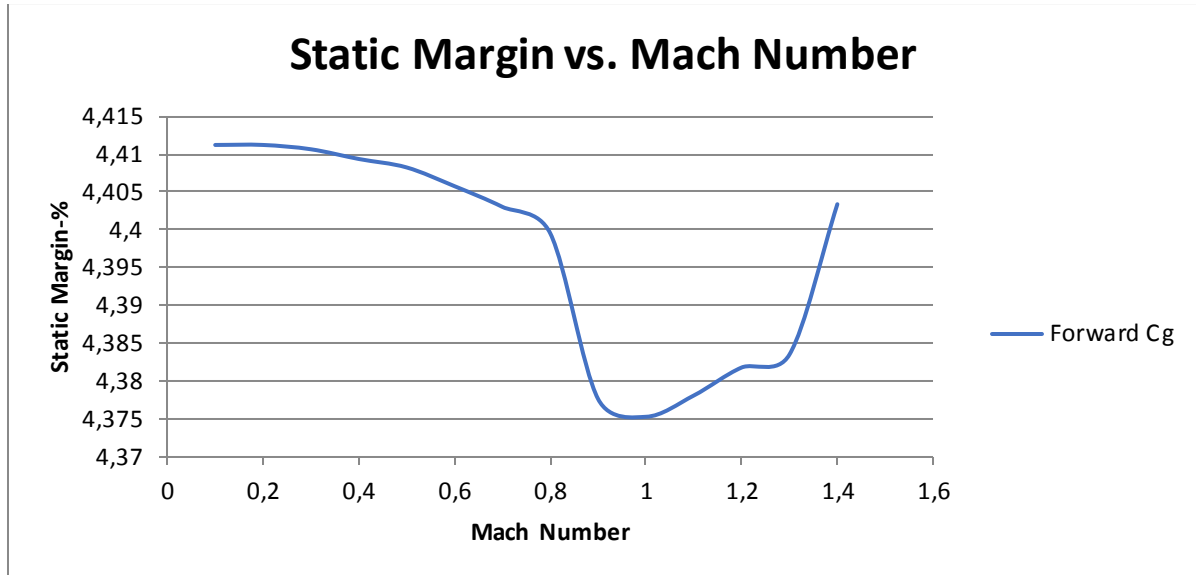


*Figure 52:Static Margin vs. Mach Number*

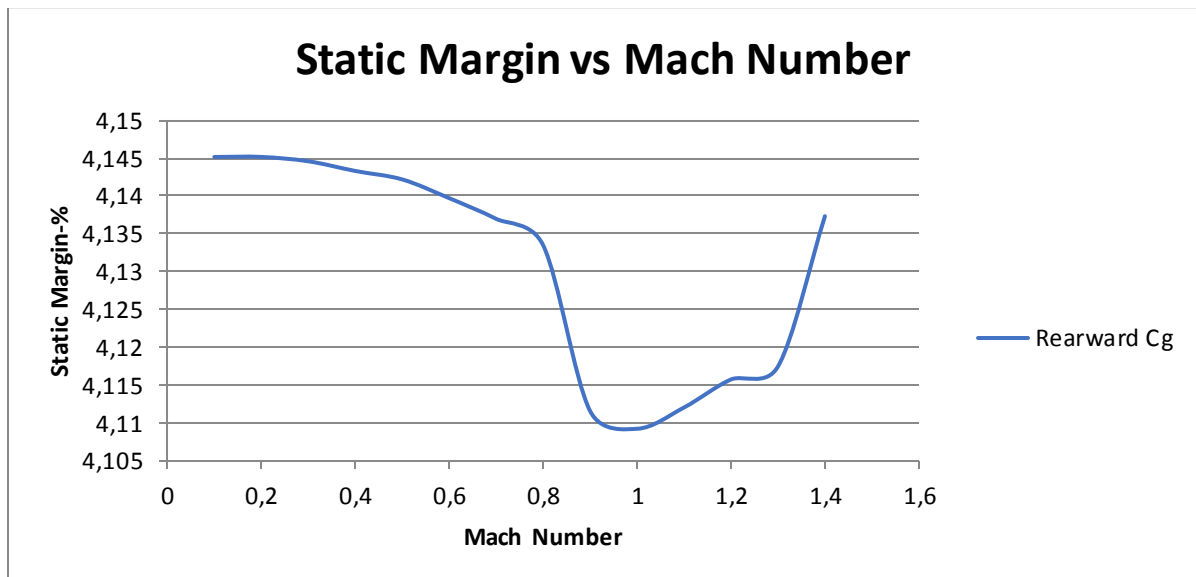


*Figure 53:Static Margin vs. Mach Number*

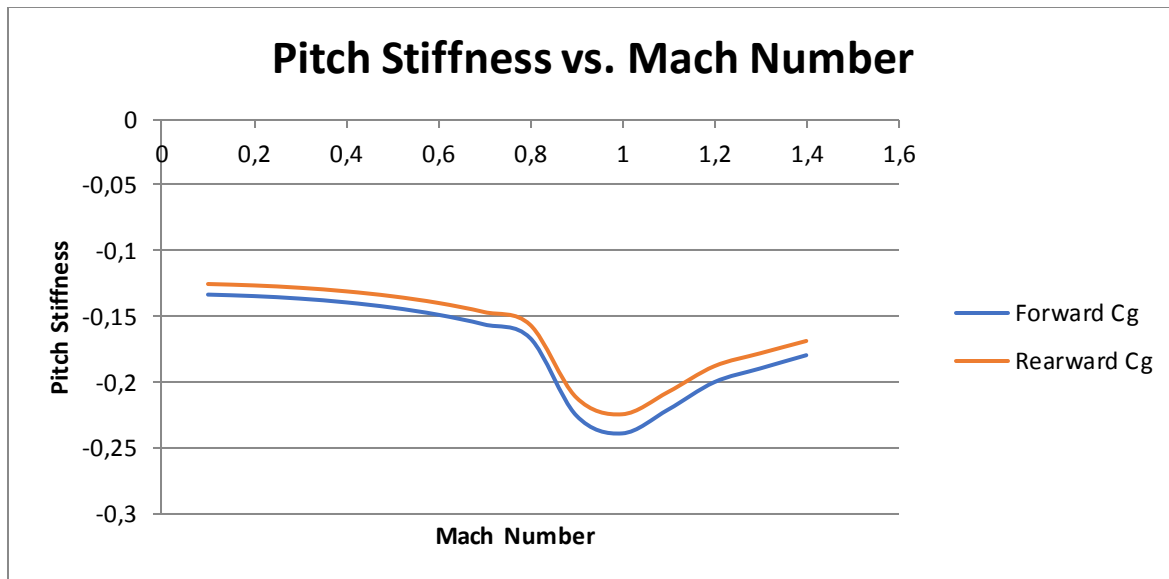


**Figure 54:** Pitch Stiffness vs. Mach Number

## CONCLUSION

Aviation comes into prominence day by day. For military jet trainer aircraft high speed, high engine thrust, stealthiness, better range, high manoeuvre capability is the most important parameters and the aircraft was designed taken into consideration these capabilities.

Design process is started with the observation of the similar type of competitor aircraft. Required data of competitor aircraft was obtained and database was formed. Weight estimation was conducted according to given design requirement. Secant method was used for initial estimation of the aircraft weight. Then, airfoil was selected according to required performance requirements and mission. Taken into consideration of the requirements engine was selected. Component of aircraft such as wing, fuselage, tail, control surfaces, landing gear type are determined and sized. While determining the precise value of the wing, fuel tank volume was taken into consideration. After sizing process, aircraft was drawn on the SolidWorks in a detail way and better weight estimation was conducted and most forward and rearward cg was estimated for different types of weapons. Performance calculation was conducted. Then, take-off and landing distance was carried out. V-n diagram was obtained and corner velocity was defined. Finally, cost analysis was conducted and stability analysis was performed.

The manufacturing process started for the aircraft after design steps which was mentioned above.

## REFERENCES

- [1] [https://www.militaryfactory.com/aircraft/detail.asp?aircraft\\_id=22](https://www.militaryfactory.com/aircraft/detail.asp?aircraft_id=22)
- [2] <https://www.fighter-planes.com/>
- [3] [https://www.militaryfactory.com/aircraft/detail.asp?aircraft\\_id=513](https://www.militaryfactory.com/aircraft/detail.asp?aircraft_id=513)
- [4] <https://www.aircraftcompare.com/helicopter-airplane/Lockheed-Martin-T50-Golden-Eagle/172>
- [5] <https://www.airforce-technology.com/projects/t-50/>
- [6] <https://ndiastorage.blob.core.usgovcloudapi.net/ndia/2002/gun/cromack.pdf>
- [7] <https://alchetron.com/KAI-T-50-Golden-Eagle>
- [8] [http://www.flugzeuginfo.net/acdata\\_php/acdata\\_t50a50\\_en.php](http://www.flugzeuginfo.net/acdata_php/acdata_t50a50_en.php)
- [9] [http://www.koreaaero.com/english/product/fixedwing\\_t-50.asp](http://www.koreaaero.com/english/product/fixedwing_t-50.asp)
- [10] [https://www.militaryfactory.com/aircraft/detail.asp?aircraft\\_id=232](https://www.militaryfactory.com/aircraft/detail.asp?aircraft_id=232)
- [11] [http://www.mirage-jet.com/COMPAR\\_1/compar\\_1.htm](http://www.mirage-jet.com/COMPAR_1/compar_1.htm)
- [12] <https://www.airforce-technology.com/projects/mirage/>
- [13] [https://www.forecastinternational.com/archive/dispatch\\_pdf.cfm?DACH\\_RECNO=252](https://www.forecastinternational.com/archive/dispatch_pdf.cfm?DACH_RECNO=252)
- [14] Jackson, Paul; (2004–2005). "*Jane's All the World's Aircraft*", pp. 135
- [15] <http://idrw.org/why-hal-plans-to-convert-lca-trainer-into-lead-in-fighter-trainer-lift-for-export/>
- [16] <http://www.tejas.gov.in/ADA-Tejas%20Brochure-2015.pdf>
- [17] <https://www.quora.com/What-are-the-specs-of-Tejas-Mk-1A>
- [18] Jackson, Paul; Peacock, Lindsay; Bushell, Susan; Willis, David; Winchester, Jim, eds. (2016–2017). "*Jane's All the World's Aircraft: Development & Production. Coulson.*" pp. 302–303
- [19] [http://tejas.gov.in/specifications/leading\\_particulars\\_and\\_performance.html](http://tejas.gov.in/specifications/leading_particulars_and_performance.html)
- [20] <https://www.drdo.gov.in/drdo/pub/techfocus/2011/feb%202011%20.pdf>
- [21] <https://www.naval-technology.com/projects/hal-tejas/>
- [22] <https://www.quora.com/Whats-limiting-the-LCA-Tejas-performance-to-half-the-payload-and-endurance-of-the-SAAB-Gripen-and-F-16>
- [23] Jackson, Paul; (2004–2005). "*Jane's All the World's Aircraft*", pp. 82
- [24] [https://www.militaryfactory.com/aircraft/detail.asp?aircraft\\_id=363](https://www.militaryfactory.com/aircraft/detail.asp?aircraft_id=363)
- [25] <https://www.airforce-technology.com/projects/f2/>
- [26] <https://www.flightglobal.com/news/articles/big-in-japan-tokyos-top-10-aircraft-projects-405209/>
- [27] Jackson, Paul; (2004–2005). "*Jane's All the World's Aircraft*", pp. 333
- [28] <https://www.airforce-technology.com/projects/gripen/>
- [29] <https://www.bilgiustam.com/jas-39-gripen-savas-jeti/>
- [30] [http://aviationweek.com/site-files/aviationweek.com/files/uploads/2014/09/asd\\_09\\_25\\_2014\\_jas7.pdf](http://aviationweek.com/site-files/aviationweek.com/files/uploads/2014/09/asd_09_25_2014_jas7.pdf)
- [31] <https://www.lockheedmartin.com/en-us/products/f-16.html>
- [32] <https://www.airforce-technology.com/projects/f16/>
- [33] <https://www.aircraftcompare.com/helicopter-airplane/lockheed-martin-f16-fighting-falcon/169>
- [34] Sadraey, M.H., *Aircraft Design A System Engineering Approach*, 2nd ed., A John Wiley & Sons, Ltd. Publication, New Hampshire, 2013

- [35]Raymer, D.P., *Aircraft Design: A Conceptual Approach*, 2nd ed., American Institute of Aeronautics and Astronautics, Washington, 1992
- [36]John D. Anderson, *Aircraft Performance and Design* 2nd Ed. Mc Graw Hill. 1999
- [37]B. Etkin, L.D.Reid. (1996). *Dynamics of Flight*. United States of America: John Wiley and Sons Inc.
- [38]Roskam, J. (1985). *Airplane Design*
- [39]Tulapurkara, E. *Longitudinal Stick- Fixed Static Stability and Control*

## NOMENCLATURE

$W_0$	Maximum Takeoff Weight
$W_{crew}$	Crew Weight
$W_{payload}$	Payload Weight
$W_f$	Fuel Weight
$W_e$	Empty Weight
$R$	Range
$E$	Endurance
$C$	Specific Fuel Consumption
$d$	Duration
$C_l$	Lift Coefficient of Airfoil
$C_d$	Drag Coefficient of Airfoil
$C_m$	Moment Coefficient of Airfoil
$C_{lmax}$	Maximum Lift Coefficient of Airfoil
$C_{dmin}$	Minimum Drag Coefficient of Airfoil
$Re$	Reynolds Number
$L$	Lift
$W$	Weight
$T$	Thrust
$D$	Drag
$V_s$	Stall Speed
$\rho$	Density
$S$	Wing Area
$L/D$	Lift to Drag Ratio
$AR$	Aspect Ratio
$C_r$	Root Chord
$C_t$	Tip Chord
$\lambda$	Taper Ratio
$\Gamma$	Dihedral Angle
$b_{VT}$	Vertical Tail Span
$Cr_{VT}$	Vertical Tail Root Chord
$Ct_{VT}$	Vertical Tail tip Chord
$b_{HT}$	Horizontal Tail Span
$Cr_{HT}$	Horizontal Tail Root Chord
$Ct_{HT}$	Horizontal Tail tip Chord
$\alpha$	Angle of Attack
$b$	Span
$cg$	Center of Gravity
$\bar{c}$	Mean Aerodynamic Chord
$V_{HT}$	Horizontal Tail Volume Ratio
$I_{HT}$	Horizontal Tail Moment Arm
$S_{HT}$	Horizontal Tail Area
$S_{VT}$	Vertical Tail Volume Ratio
$S_{wet}$	Wetted Area
$W/S$	Wing Loading
$V_\infty$	Free Stream Velocity
$H_{LG}$	Landing Gear Height
$Ac$	Capture Area
$\dot{m}$	Mass Flow

$H_f$	Fuselage Height
$\alpha_c$	Clearance Angle
$\alpha_{TO}$	Take-off Rotation Angle
$\Phi_{ot}$	Overturn Angle
$Y_{ot}$	Wheel Track Distance
$W_W$	Wheel Wight
$\eta$	Airfoil efficiency
$n$	Load Factor
$\Lambda_{LE}$	Leading Edge Sweep Angle
$\Lambda$	Sweep Angle
$L_f$	Fuselage Length
$D_f$	Fuselage Diameter
$x_{cg}$	Horizontal Center of Gravity Location
$z_{cg}$	Vertical Center of Gravity Location
$M$	Mach Number
$M_{crit}$	Critical Mach Number
$M_{dd}$	Mach Divergence Number
$C_{fe}$	Skin Friction Coefficient
$C_{D_0}$	Parasite Drag
$S_{ref}$	Reference Area
$e$	Oswald Span Efficiency
$P_R$	Power Required
$P_A$	Power Available
$T_R$	Thrust Required
$T_A$	Thrust Available
$R/C$	Rate of Climb
$S_{Landing}$	Landing Distance
$S_{TO}$	Take-off Distance
$X_{np}$	Neutral Point
$H_Q$	Quality Control Hours
$H_E$	Engine Hours
$H_T$	Tooling Hours
$H_M$	Manufacturing Hours
$C_D$	Devel Support Hours
$C_F$	Flight test Cost
$C_M$	Manufacturing Materials Cost
$C_{eng}$	Engine Production Cost
$R_T$	Tooling Wrap Rates
$R_E$	Engineering Wrap Rates
$R_M$	Manufacturing Wrap Rates
$R_Q$	Quality Control Wrap Rates
$N_{eng}$	Total Production Quantity Times times number of engine per aircraft
$C_{avionics}$	Avionics Cost
$FTA$	Number of Flight Test Aircraft
$Q$	Production Quantity
$C_{L\alpha}$	Airplane lift-curve slope
$X_{acw}$	Aerodynamic Center Wing Body

$C_{m_{\alpha fus}}$	Pitching Moment Fuselage
$\eta_h$	Tail Dynamic Pressure Ratio
$C_{L_{\alpha h}}$	Tail lift-curve slope
$X_{ach}$	Aerodynamic Center Tail
$Fp_{\alpha}$	Derivative of Normal Force with Respect to Angle of Attack
$K_f$	Emprical Pitching Moment Factor
$L_f$	Length of Fuselage
$W_f$	Width of the Fuselage